Copyright Warning & Restrictions

The copyright law of the United States (Title 17, United States Code) governs the making of photocopies or other reproductions of copyrighted material.

Under certain conditions specified in the law, libraries and archives are authorized to furnish a photocopy or other reproduction. One of these specified conditions is that the photocopy or reproduction is not to be "used for any purpose other than private study, scholarship, or research." If a, user makes a request for, or later uses, a photocopy or reproduction for purposes in excess of "fair use" that user may be liable for copyright infringement,

This institution reserves the right to refuse to accept a copying order if, in its judgment, fulfillment of the order would involve violation of copyright law.

Please Note: The author retains the copyright while the New Jersey Institute of Technology reserves the right to distribute this thesis or dissertation

Printing note: If you do not wish to print this page, then select "Pages from: first page # to: last page #" on the print dialog screen

ABSTRACT

DEVELOPMENT OF AN INTELLIGENT GEOMETRY MEASUREMENT PROCEDURE FOR COORDINATE MEASURING MACHINES

by

Tae-Sung Kim

A Coordinate Measuring Machines (CMM) is a highly accurate electronic scale for the automatic measurement of 2 and 3 dimensional geometries. In a typical operation the CMM measures a set of user defined points, and then utilizes some internal logic to ascertain whether the inspected part meets the specifications. CMMs have received widespread acceptance among the manufacturing community, and in many instances are required as per supplier contract. Applications of CMMs vary from the measurement of simple 2D parts to complex 3D spatial frames (as for example in their use to measure the integrity of automobile frames). The primary objective of the proposed research is to investigate procedures for the efficient use of CMMs.

Two of the key parameters in CMM usage are the number of points measured, and the relative location of the points measured. In this thesis we firsts show that when these two inspection parameters are varied, for the same part, then different conclusions with regard to the part's geometry may be drawn. Next we investigate the relationship between these two parameters and the reliability of the concluded data. Specifically we focus on a 2D circle, a 2D rectangle, and a 2D plane. The experiments were conducted on the Brown & Sharpe's Coordinate Measuring Machine.

DEVELOPMENT OF AN INTELLIGENT GEOMETRY MEASUREMENT PROCEDURE FOR COORDINATE MEASURING MACHINES

by
Tae-Sung Kim

A Thesis
Submitted to the Faculty of
New Jersey Institute of Technology
in Partial Fulfillment of the Requirements for the Degree of
Master of Science in Industrial Engineering

Department of Mechanical and Industrial Engineering

October 1993

APPROVAL PAGE

Development of an Intelligent Geometry Measurement Procedure for Coordinate Measuring Machines

Tae-Sung Kim

Dr. Sanchoy K. Das, Thesis Adviser — date
Assistant Professor of Industrial and Management Engineering
New Jersey Institute of Technology

Dr. Xiuli Chao, Committee Member — date
Assistant Professor of Industrial Engineering
New Jersey Institute of Technology

Dr. Raj Sodhi, Committee Member — date
Associate Professor of Mechanical Engineering
New Jersey Institute of Technology

BIOGRAPHICAL SKETCH

Author: Tae-Sung Kim

Degree: Master of Science in Industrial Engineering

Date: October 1993

Undergraduate and Graduate Education:

- Master of Science in Industrial Engineering, New Jersey Institute of Technology, Newark, NJ, 1993
- Bachelor of Science in Industrial Engineering, Dongguk University, Seoul, Korea, 1991

Major: Industrial Engineering

This thesis is dedicated to

Jesus Christ

ACKNOWLEDGMENT

I would like to express my sincere thanks to Dr. Sanchoy K. Das, my thesis adviser, for all the help he provided me during the preparation of my thesis. My gratitude to Dr. Sanchoy K. Das who was the source of many ideas which helped me to develop the model. I learned many things during my discussions with him which will help me in continuing further research in this topic. I would respectfully like to extend my gratitude to Dr. Xiuli Chao and Dr. Raj Sodhi who helped me in developing mathematical equations correctly and suggesting many ideas to make the thesis worth presenting in the present form, as well as for future work. Many thanks to Alan Bondhus and Michael Onofrietto of Center for Manufacturing Systems, NJIT, who provided the experimental data without which the verification of correctness of theoretical results would not have been possible.

I further thank Rev. Henry W. Nelson, Tae-Quin Kim and Hyun-Hue Kim for their suggestions and support during correction time at church and school.

Finally I must say that it was a great fun to think together, to fight together during discussions and enjoy together the results obtained in this thesis. Thanks again to the members of the team for creating this type of congenial atmosphere.

TABLE OF CONTENTS

Chapter **Page**

Chapter **Page**

LIST OF TABLES

Table **Page**

LIST OF FIGURES

Figure **Page**

Figure **Page**

CHAPTER 1

INTRODUCTION

1.1 Introduction

Modern manufacturing processes for discrete parts require fast and accurate measuring devices to check critical dimensions against their specified values. As demands for better quality assurance, faster turnaround time and lower production costs continue to increase, so does the use of coordinate measuring machines (CMMs) for inspection operations. Advantages such as enhanced accuracy, reduced inspection time and better equipment utilization are just some of the reasons for the growing use of CMMs.

With the advent of numerically controlled NC machine tools, mainly mills and drills, demand has grown for a means to support NC production with faster, first-piece inspection, and in many cases, 100 % inspection. To fill this need, coordinate measuring machines (CMMs) were developed by modifying precision layout machines. In effect, most CMMs can be used as layout machines before machining and for the checking of hole locations after machining. Thus the CMM plays a vital role in the mechanization of the inspection process.

There are many types of CMM. Cantilever is the easiest to load and unload, but it is the most susceptible to mechanical error because of sag (deflection) in the Y axis beam. The bridge type is less sensitive to mechanical errors, but more difficult to load. The horizontal bore mill type is best suited for large, heavy workpieces. The floating bridge is a compromise between cantilever and bridge. It is fast to operate, alignment is simple, and rugged construction affords consistent accuracy.

For these reasons the relatively recent development of the modern CMM represents a significant contribution to the state of the art of dimensional metrology. Built to facilitate the inspection of discrete piece parts, the machine has improved the quality

and reliability of measurement data and has reduced inspection time by as much as 80 percent. CMMs are manufactured in both manual and automatic (computer-controlled) models and come in a wide range of sizes to accommodate a variety of applications.

Since the measuring probe can be moved manually from point to point and the measurement data is displayed on the readout at a very brisk pace in most cases, the automatic recording and processing of data is essential to full utilization of the machine's potential. The complexity of the computation required will vary with different measurements, ranging from a simple calculation of difference between actual and nominal coordinates to complex geometric and statistical analyses.

Although the incorporation of automatic on-line data processing increased the utilization of CMM's, there still remains the problem of operator-induced errors in the inspection of complex parts, and parts with numerous dimensional features. Machine operators subject to distraction which measuring numerous similiar or dissimliar component features. This will seriously damage if consistency of measurement which can only be achived autometic control.

It is impossible to manufacture a mechanically perfect machine. It is important to be able to analyze the geometry errors associated with individual precision CMMs and to determine their effects on the machine's measurement accuracy. The results of such analyses can be used to compensate for these effects and thus to provide a degree of accuracy that could not otherwise be achieved.

The accuracy of CMMs and machine tools depends on the accuracy of the position transducers on the linear and rotary moving axes and on the geometric accuracy of the motion of these axes. In the past, high-precision machines have been so designed that the geometry of the various motions could be adjusted during assembly to achieve a required level of accuracy. More recently machine-precision requirements have become so stringent that such an adjustment is not always sufficient. Instead it is necessary to

analyze the geometry errors involved and to determine their effects on the machine's measurement accuracy.

Reliable estimates of overall machine accuracy can be made in the design stage, based on the accuracy of the measurement transducers and on the deviation of the actual position of the gauging probe from the position indicated by the transducer readouts. Such an estimate assits in one to predict machine specifications, to determine whether design changes are necessary to achieve the level of accuracy that will be required, and to set up a tolerance budget for use during design and manufacture. Geometric-error analysis also makes it possible to compensate for the effects on these errors, either by introducing mechanical design features or by adding external data-handling systems capable of upgrading the measurement accuracy of the machine. If machine geometry is mapped to determine repeatable errors, data can be stored that will make the necessary corrections. Errors that are not repeatable cannot be corrected for in this manner, but instead must be continually monitored if correction is necessary. In certain case's error signals can be made to drive servos that will correct machine geometry, though more often than not this method of correction is impractical.

The task is to calculate, for each machine configuration of interest, the actual position of the gauge tip relative to the machine datum point in terms of the position indicated by the measurement transducers and the geometry errors. In addition, it is useful to determine the uncertainty in actual position in terms of the uncertainties in the position-transducer indications and geometry error measurements. The calculations must include every sensitive error possible, every deviation from the desired motion that cause the tool or gauge tip to move in the measurement direction. Any motion that causes the tool to move in a direction normal to the desired motion is insensitive since its effect on the actual position of the tip is usually negligible.

An inspection planning procedure is created. The inspection planning procedure can assist process designers in determining an initial inspection plan based on

manufacturing process capability, assigned geometric error and inspection accuracy requirements.

If the geometric form of the part surface is perfect, the coordinate estimation based on enough number of discrete points, will be exact. On the surface of any real part, however, geometric errors always exist. They appear in a continus manner. Therefore, the result of coordinate estimation depends on the number and locations of the discrete points being used. In other words, when using discrete coordinates, variations of coordinate estimation should be expected as long as geometric errors exist.

In manufacturing, this might result in the production of products that are out of tolerance. In inspection, this might lead to the wrong decision of acceptance or rejection of the inspected part. Therefore, for the quality assurance of high precision engineered products, the coordinate measuring points must be analyzed.

For inspection planning, some research has been conducted on the generation of collision-free inspection path [Yau and Menq, 1991; Lim, 1992]. However, little research has addressed the problem of determining the number and locations of the required measurement points. The determination of measurement points is a rather complicated problem. It is believed that the number and locations of the required measurement points would depend on various factors of relevance to design specification, manufacturing processes and requirements for inspection accuracy. Menq et al.[1992] proposed a method to determine the number of measurement points for the inspection of form tolerance based on a statistical analysis. This research is a good starting point for studying inspection planning. However, there are two limitations of these works. First, the geometric error on the part surface is assumed to follow a normal distribution. In reality, not only the real error distribution will be different from a normal distribution in some degree, but also the variation of geometric form fitting will influence on the results of tolerance evaluation. In current practice of dimensional inspection, there are no guidelines available for selecting the number and locations of measurement points.

1.2 Research Objectives

There two primary research objectives in this thesis. These are:

(a) To identify and characterize the type of errors made by a CMM when measuring geometrical shapes.

(b) To design an inspection procedure, that is the number and location of measured point, so as to optimize the reliality of the inspection process.

This study formulate an optimization algorithm to analyze the measured coordinates' data. The algorithm is labelled GMP/C. The current study deals with geometric features and geometric tolerances. The analytical procedures, which deal the size tolerance and different geometric errors, that are round, straight, flat, angle and perpendicular. How many points are needed to inspect the product reliably? Which points should be measured? What should be the sampling size on a production line? Should the identical points be measured on all inspected products? These are all the deviations related to a circle, rectangle, and polygon.

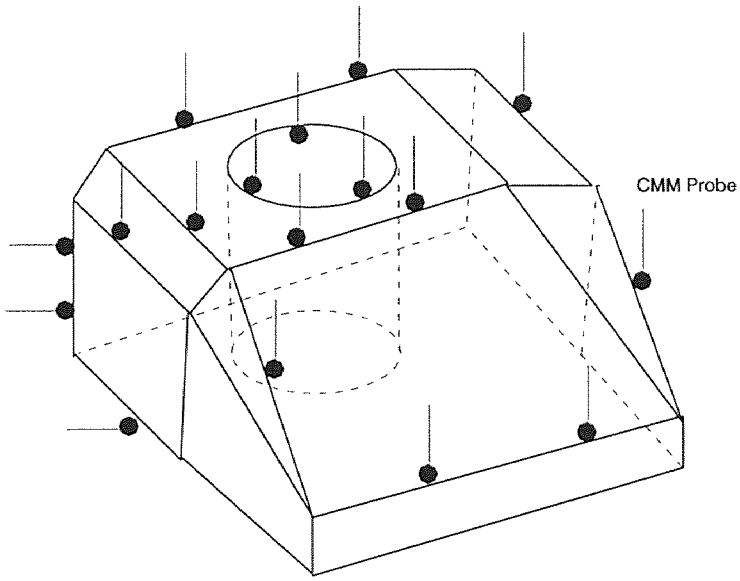

Figure 1.1 The Diagram of using a CMM to Inspection Parts

When the measuring procedure is completed, the data input to the CMM Geometry Measurement Procedure (GMP/C) is a design data file. The user then specifies

which geometric in the design are to be inspected, what is the required reliability and accuracy, and finally how the part is manufactured. The GMP/C analyze the input data and determine which points (and how many points) in the geometry should be measured, further it will specify what the inspection sample size should be. As part of the seed money project we are concentrating on simple 2-D geometric such as circles, rectangles, and polygons.

The objective of this thesis is to develop an intelligent procedure for the efficient use of Coordinate Measuring Machine (CMM). A CMM is basically a highly accurate electronic scale for the automatic measurement of 2 and 3 dimensional geometry. In a typical operation, the CMM measures a set of user defined points, and then utilizes some internal logic to ascertain whether the inspected part meets the specifications. This configuration is shown in figure 1.1. One significant disadvantage of a CMM is that it is a point measuring device, and hence unable to utilize measurement tools such as V-blocks, go/nogo blocks, calipers, etc. Further, it is left to the user to specify to the machine which points are to be measured.

1.3 Thesis Organization

This thesis organized as follows: Chapter 2 describes the coordinate measuring machine. There are advantages of using coordinate measuring machines in section 2.6. A review of research about coordinate measuring machines presented in section 2.7. Chapter 3, modeling of coordinate measuring machine is described as a function of the number of measured point. Chapter 4 describes the experimental analysis of CMM model. Chapter 5 states the conclusion.

CHAPTER 2

COORDINATE MEASURING MACHINES

Market saturation and the pressure of worldwide competition are forcing firms today to manufacture products of higher quality and performance without rising production costs. At the same time there is a demand for even more customer orientation, i.e., a greater variety of products made in smaller quantities.

This can only be achieved by a higher degree of automation in production and quality control. While automatic inspection routines have been state-of-the-art for many years, the automatic measurement center where even component feed and the choice of part program are computer-controlled.

The primary consequences for us as manufacturer are to offer future oriented solutions to problems in dimensional metrology that are geared to specific customer requirements, grow with changing needs and can easily be put into practice. An important aspect is compatibility of hardware and software, so that your investment in the solution of today's measuring problems forms the basis for future success as well. Coordinate measuring machine(CMM) offers a carefully matched range of hardware and software components for production and quality control.

2.1 Coordinate Measuring Machine Approach

CMM has used in one of three ways in a manufacturing firm. There are three approaches in manufacturing firms. First, the CMM at the end of the production line or in an inspection area. With this approach, the CMM is used to inspect the first part of a production run to verify the machine setup. Once the setup is verified, it then measures parts on a random basis.

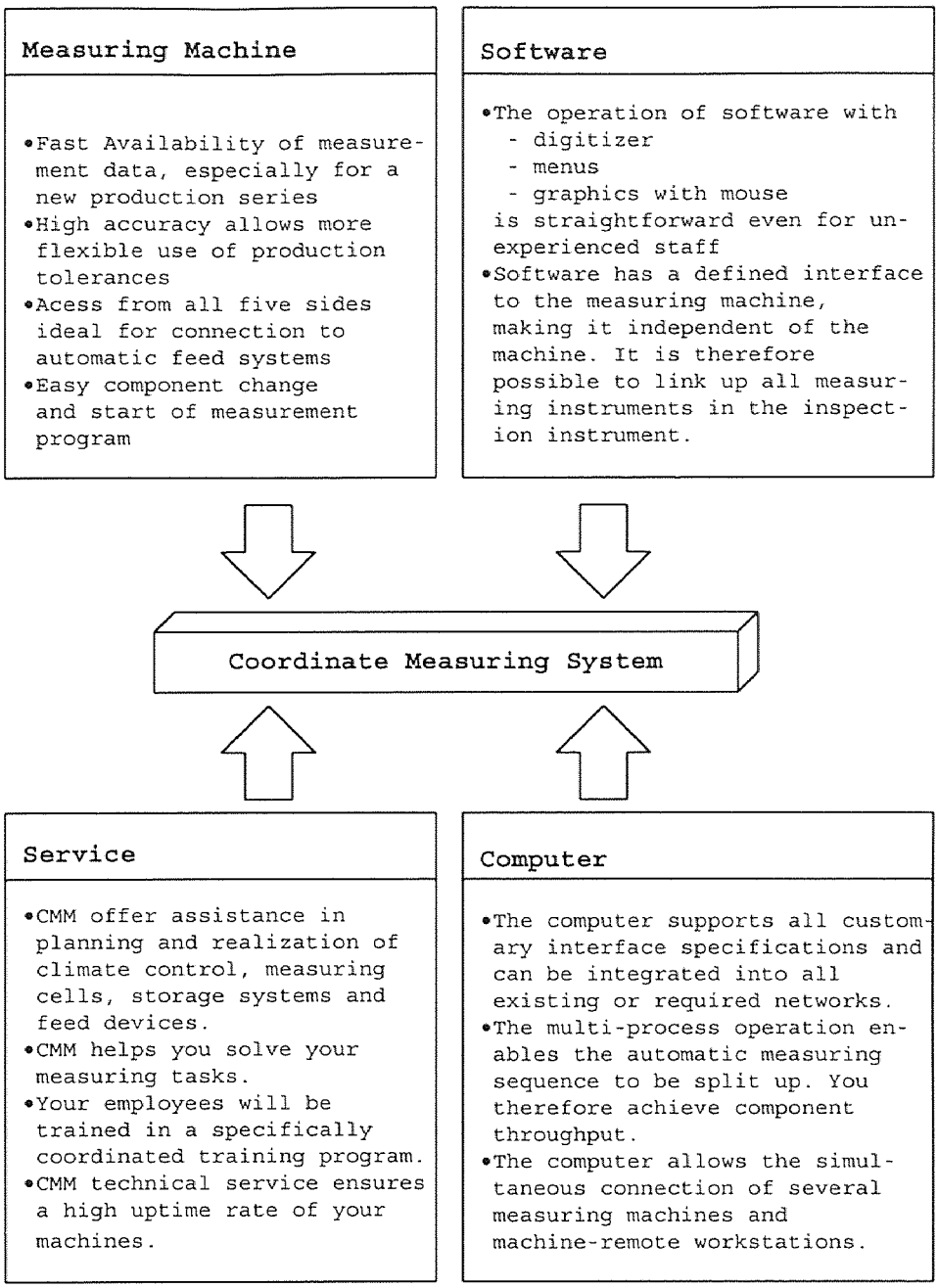

Figure 2.1 Diagram of the Coordinate Measuring System

Second approach is to incorporate the CMM between two work centers and then measure 100% of the parts produced at the first center before any secondary operations are performed at the second work center. This approach is possible because CMMs are capable of measuring three-dimensional geometry and making many different measurements within a short period of time. When this approach is used, the CMM indirectly controls the production process.

A third approach integrates the CMM into the production line. This permits the CMM to directly control the production process. In operation, an integrated system would measure the workpiece, compare the measurements with required dimensions, and, if necessary, automatically adjust the machine controls so that the part is manufactured within the required specifications.

2.1.1 A Basic Coordinate Measuring Machine

(1) The machine structure, which basically is an X-Y-Z positioning device

(2) The probing system used to collect raw data on the part and provide input to the control system

(3) Machine control and computer hardware

(4) The software for three-dimensional geometry analysis

2.1.2 Machine Configurations

A variety of machine configurations are available from the manufacturers of CMMs. Each configuration has advantages that make it suitable for particular applications.

(a) Cantilever

Cantilever-type CMMs are usually the smallest in size and the lowest in cost, and occupy a minimum of floor space. This configuration permits a completely unobstructed work area, allowing full access to load, inspect, and unload parts that may be larger than the table.

It also provides convenient, close grouping of machine controls. The single overhanging beam support for the probe head may limit accuracy if a special compensation is not built into the cantilever arm. The movement of the probe from one inspection point to another is usually performed manually by the machine operator; however, joystick and CNC machines are available. The machine of this configuration is shown in Figure 2.2, (a).

(b) Bridge

Bridge-type coordinate measuring machines employ three movable components moving along mutually perpendicular guide ways. The probe is attached to the first component, which moves vertically (Z direction) relative to the second. The second component moves horizontally (Y direction) relative to the third. The third component is supported on two legs that reach down to opposite sides of the machine base and moves horizontally (X direction) relative to the base. The workpiece is supported on the base. This configuration is shown in Figure 2.2, (b).

The bridge-type CMM is the most popular configuration. The double-sided support of this type of CMM provides more support for large and medium-sized machines. The bridge can slide back on the base to give complete accessibility to the working area for safe, easy loading and unloading of parts.

(c) Column

Column-type CMMs are similar in construction to accurate jig boring machines. The column moves in a vertical (Z) direction only, and two-axis saddle permits movement in the horizontal (x and Y) direction.

Column-type CMMs are often referred to as universal measuring machines rather than CMMs by manufacturers and are considered gage-room instruments rather than production-floor machines. This configuration is shown in Figure 2.2, (c).

(d) Gantry

Gantry-type CMMs employ three movable components moving along mutually perpendicular guide ways. The probe is attached to the probe quill, which moves vertically (Z direction) relative to a cross beam. The probe quill is mounted in a carriage that moves horizontally (Y direction) along the cross beam. The cross beam is supported and moves in the X direction along two elevated rails, which are supported by columns attached to the floor.

The gantry-type configuration was initially introduced in the early 1960s to inspect large parts such as airplane fuselages, automobile bodies, ship propellers, and diesel engine blocks. The open design permits the operator to remain close to the part being inspected while minimizing the inertia of the moving machine parts and maintaining structural stiffness. This configuration is shown in Figure 2.2, (d).

(e) Horizontal Arm

The horizontal arm configuration employs three movable components moving along mutually perpendicular guide ways. In the moving-ram design, the probe is attached to the horizontal arm, which moves in a horizontal Y direction. The ram is encased in a carriage that moves in a vertical (Z) direction and is supported on a column that moves horizontally (X direction) relative to the base.

Horizontal arm CMMs are used to inspect the dimensional and geometric accuracy of a broad spectrum of machined or fabricated workpieces. Utilizing an electronic probe, these machines check parts in a mode similar to the way they are machine on horizontal machine tools.

They are especially suited for measuring large gear cases and engine blocks, where high-precision bore alignment and geometry measurements are required, By incorporating a rotary table, four-axis capability is obtainable. This configuration is shown in Figure 2.2, (e).

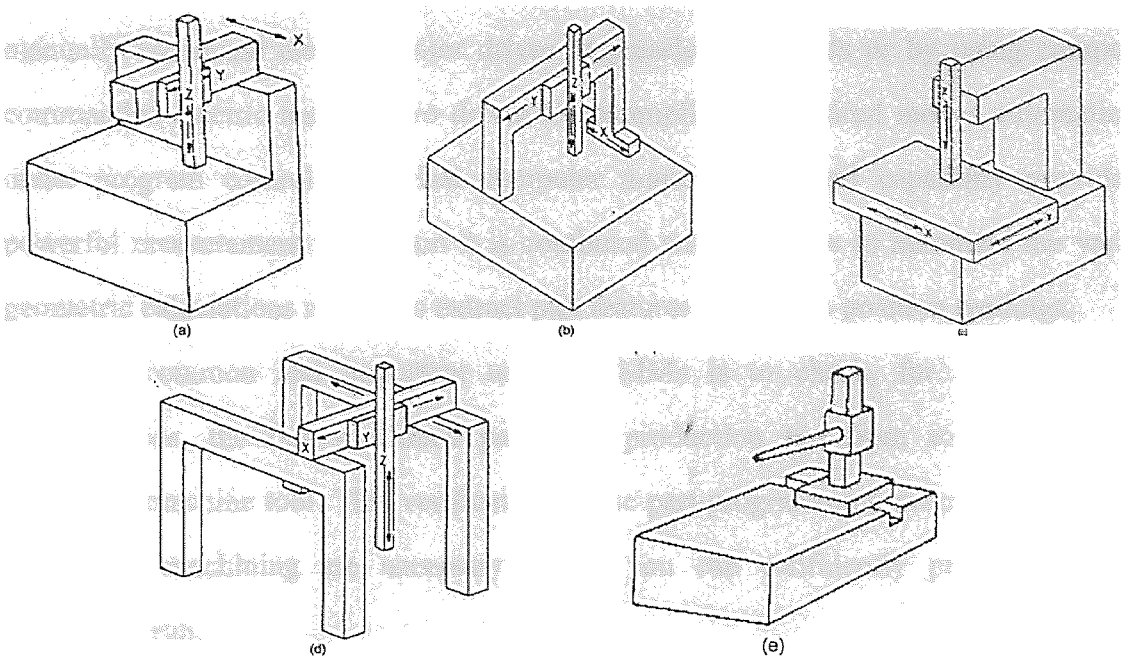

Figure 2.2 The Type of Coordinate Measuring Machines

2.2 Probe

The probe is used only to provide a sensitive and reproducible indication of when the probe touches the measured part; the three-dimensional position of the probe is actuarially read from the slide-position transducers on each machine axis. Thus to measure the width ω of the part shown in Figure 2.3, we drive the slide from position ① in the negative x directions until contact is made, at which instant the x, y, z readings will be "frozen" so that we (or a machine memory) can record them. Then we move the slide to position ② (same y and z readings as position ①) and drive it in the positive x direction until a "touch" signal again freezes the readings. Knowing the diameter of the probe's spherical trip, we can easily calculate ω from the difference among the two x readings.

In the actual CMM, the probe may be positioned anywhere in the working space manually (air bearings and z-axis counterweights allow you to grasp the probe body in

one hand and easily move all three slides where you wish), by using a joystick control to manually command electric motor drives at preselected speeds or by using computer-commanded electric motor servo drives to accomplish the desired moves automatically under program control. This last computer numerical control capability provides a powerful measurement tool when it is combined with software to automate the various geometric calculations needed to extract part features from slide-position readings.

A common and important use of CMMs is to check, for conformance to specifications, the first machined part in a production run from some numerically controlled machine tool. This verification of the part-programming process and all other aspects of machining are necessary before you can confidently proceed with the production run.

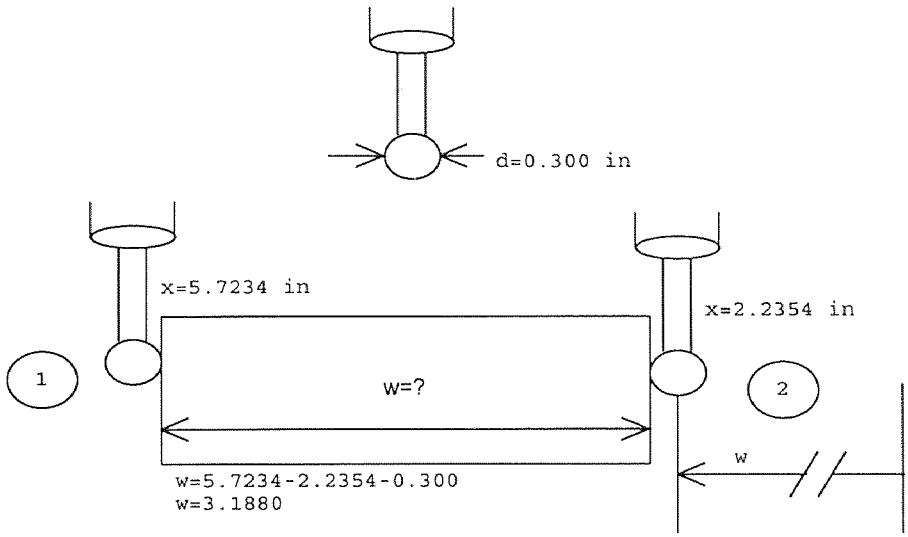

Figure 2.3 Simple Dimension Measurement with Touch Probe

2.3 Probe System

The accuracy of the measurement data and the universal application potential of CMM depend to a large extent on their measuring probe system. A CMM probes head measures the deflection in x, y and z direction when probing a workpiece and is therefore called a measuring probe system.

2.3.1 Main Construction Features

a) The deflection of the probe system is recorded electromagnetically with high resolution (differential transformers with moving core)

b) Parallel motion is achieved for all three axes with spring parallelograms.

c) The patented force-path characteristic ensures a large safety margin without large forces acting on the workpiece.

d) When work is carried out on the probe head (probe change) all axes can be clamped to protect the probe system.

2.3.2 Advantages

a) Measurement without clamping of the axes.

b) A workpiece surface with random spatial orientation can be probed vectorially from an equally random direction.

c) The deflection of the workpiece surface and the actual direction of the surface normal is detected for each probe point.

d) The measuring force is produced in proportion to the deflection and also acts perpendicularly to the workpiece surface.

e) Each time a measurement point is recorded, the deflection of the probe system in all axes is determined and stored. The bending of the probe pin can thus be calculated and compensated.

2.3.3 Dynamic Single-Point Probing

With dynamic single-point probing, the probe system is driven back at continuous speed after a deflection, whereby the coordinates of the linear measurement systems and the values of the probe system deflection are constantly read off. A spatial characteristic is formed from these values, which can be read off for any probing force between 0 and 0.5 Newton's.

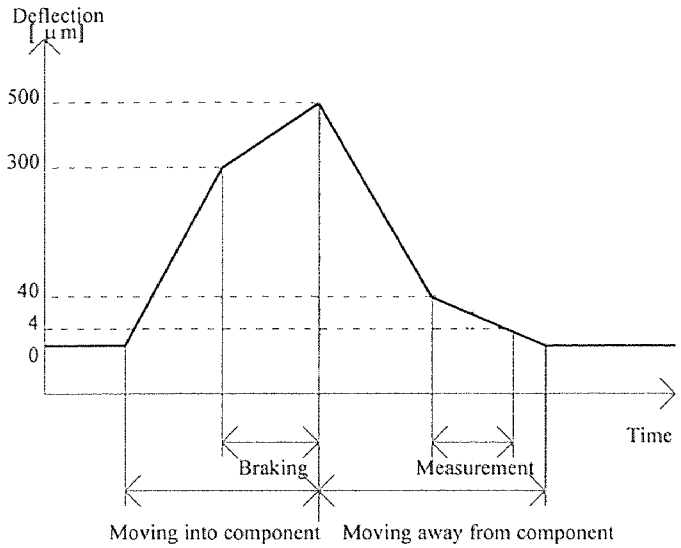

Figure 2.4 Probe Sequence

2.4 Probe Type

Three types of probes are commonly used:

(1) hard, (2) electronic, and (3) noncontact. A probe is selected according to the dimensional and geometrical requirements of the inspection process.

2.4.1 Hard Probes

Hard probes consist of a shaft and a probe tip mounted in various ways to the probe arm. A variety of probe tip shapes and sizes is available; the shape of the probe determines its application. Conical probes are used for locating holes; ball probes for establishing surface locations; cylindrical probes for checking slots and holes in sheet metal parts; and measurement of flat surfaces or edges of parts. Hard probes can only be used in small, manually operated CMMs when inspecting simple parts of a short production run.

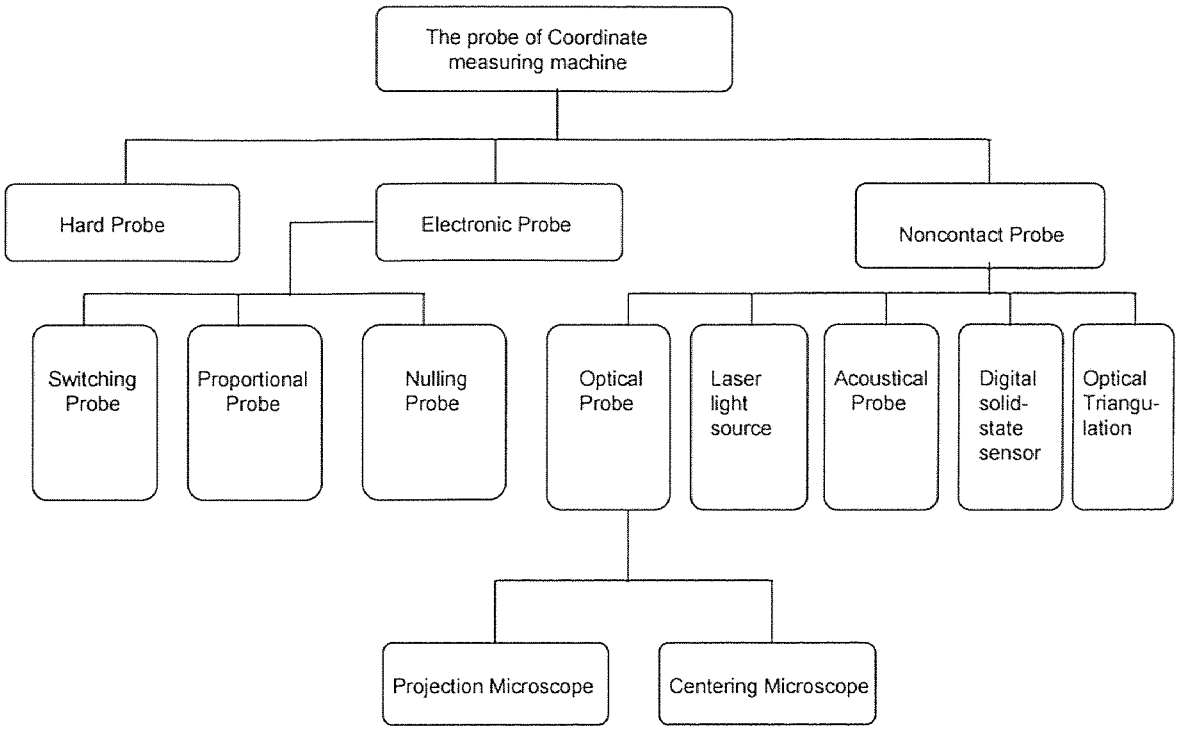

Figure 2.5 The Probe Type for Coordinate Measuring Machine

2.4.2 Electronic Probes

Electronic probes are commonly classified into one of three categories: (a) switching, (b) proportional, and (c) nulling probes.

Switching probe is the most popular probes, and is an omnidirectional triggering device consisting of a probe body and a stylus; multiple stylus arrangements are also available. When the stylus is brought into contact with the workpiece, a signal is sent to the computer interface, indicating the instantaneous three-dimensional location of the stylus.

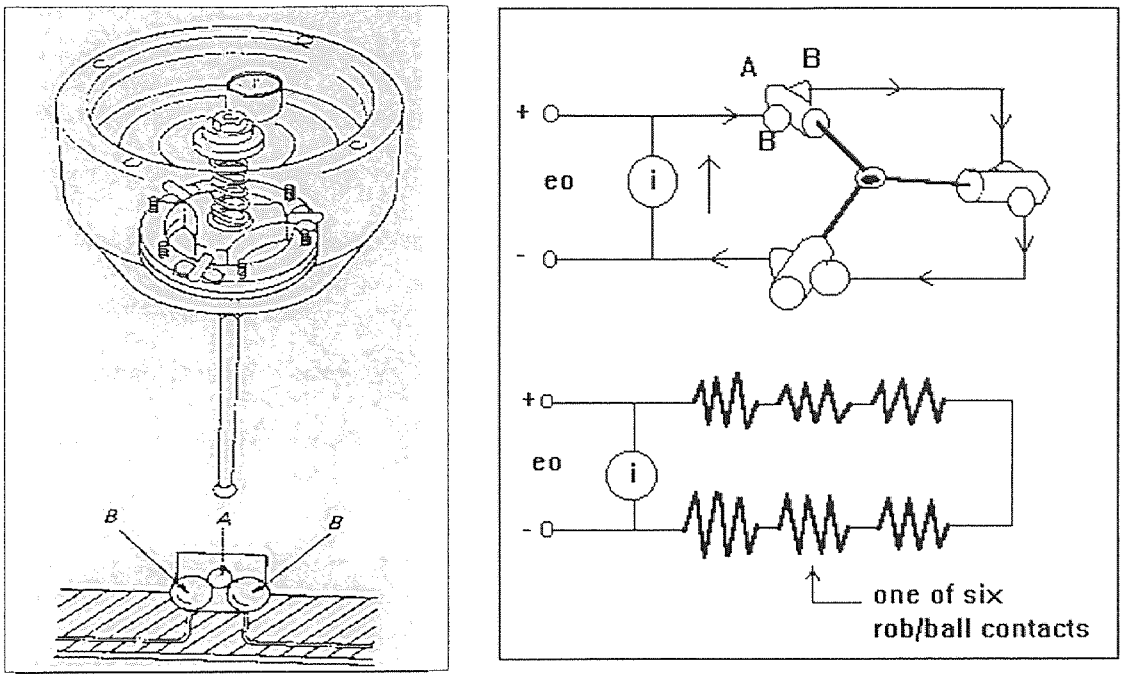

Figure 2.6 Principle of an on/off Switching Type Probe

The most widely used probe is the touch-trigger type, usable in all three machine operating modes. As explained briefly earlier, this probe is an on/off switching type which "freezes" the readings of the three slide motion sensors as the probe tip touches and is deflected by the part surface. The most common form is shown in figure 2.6. The probe stylus is kinematically located in a single unique position by the six contacts of the three cylindrical rods with the six balls, with a light spring preload maintaining this position when no external forces are applied to the stylus. The six contacts are electrically wired in series, as shown, and a constant-current source of about 0.5 mA is connected. The total resistance of the six contacts in the neutral position is on the order of a few ohms, making the voltage e_o a few millivolts. When the probe's spherical tip is deflected against the spring preload by contact with a measured part, one or more of the contact resistance's increase very greatly with tiny deflections. When the total resistance exceeds about 3000 Ω, voltage e_o passing through 1.5V trips a circuit that freezes all three slide-position readouts, recording the position of the probe at the instant of touch. A uniquely favorable

feature of the probe is its three-dimensional nature; tip deflections in $\pm x, \pm y, +z$ directions will all cause triggering, thus the probe may approach the measured part from various directions. Note that -z forces are opposed, not by the light spring preload, but by the very stiff rod-and-ball contacts. Thus the -z direction cannot be used for gaugging; however, this is rarely a problem.

All probe designs allow stylus overtravel, some by as much as 0.04" (1.0 mm) normal to probe axis and 0.08" (2.0 mm) perpendicular to the probe axis. When the deflection force is removed, the stylus returns to its initial position. Switching-type probes suffer from lobbing due to stylus bending.

This lobbing effect is exacerbated by high trigger forces and long stylus extensions. Electronic touch probes are used on all CMMs. Because of their design, proportional-type probes are used exclusively on CMMs that are controlled by direct computer control (DCC). This type of probe is designed for automatic scanning of through the probe axis. The probe consists of a transducer and a motor-powered, servo controlled axis and carries on its tip a servo-assisted feeler that generates an error signal, proportional to the pressure exerted on the part and reacts with its motor to profile variations whose amplitudes is smaller than the probe axis working stroke.

Longer profile variations are in turn followed by the CMM axes that are coupled to the probe axis position through the control system. A typical proportional probe stroke is ± 0.5" (± 12.5 mm) from the center of probe axis stroke. Other probes with simultaneous radial and axial scanning capabilities are designed with the above concept.

Nulling probes are basically the same as the proportional probe with two major differences. First of all, it is more accurate than the proportional probe because the control system indicates the three-dimensional location of the stylus when the probe is at null condition. The second major difference is that the probe must leave the surface to proceed to the next inspection location whereas the proportional probe does not.

2.4.3 Noncontact Probes

Noncontact probes are used when fast, accurate measurements are required with no physical contact with the part. Several types of noncontact probes are used.

Optical probes are used when inspecting drawings, printed circuit boards, and small, fragile workpieces. When these probes are used, the basic measuring programs can still be used.

The two types of optical probes used on manual CMMs are a projection microscope and a centering microscope. On the projection microscope, the image under inspection is displayed on the screen. Part feature locations are obtained by moving the CMM to align the screen reticule to the feature. With the centering microscope, part feature locations are obtained in the same way as the projection microscope as the user looks through the eyepiece.

Another manufacturer has developed an acoustical probe that senses contact with the workpiece by the sound wave generated by the touch rather than by any physical displacement of the probe. At contact, vibration travels up the probe and is picked up by a sensitive acoustic microphone inside the head.

A third type of noncontact probe contains a laser light source that projects a small diameter spot on the part surface. A digital solid-state sensor detects the position of this spot and computes part surface location by optical triangulation. Because of the intrinsic nature of these probes, part inspection is generally limited to two dimensions.

2.5 Probe Operation

An important detail of probe operation that was ignored in figure 2.3 is probe bending and "pretravel." The probe does not actually trigger at the instant of touch since it requires a small, but finite, force and deflection to increase the electric resistance to the 3000-Ω trigger point. Also bending deflection of the probe (minimized by using short, stiff probes whenever possible) causes a small unmeasured deflection between touching

and triggering. Fortunately, these effects are largely repeatable and may be corrected by calibration. For example, in figure 2.6 before measuring an unknown w, one would measure a precisely known w (such as a gage block), to find the "effective working diameter" d_e of the probe from the equation

$$d_e = \text{measured size - actual size}$$

Then this one d_e value can be used to correct for all three effects (ball diameters, pretravel, and bending) by using the formula

$$\text{Actual size} = \text{measured size} - d_e$$

In practice, d_e is usually found by touching a calibration sphere at about 10 points on the sphere's surface and using a special algorithm to compute d_e. This more complicated scheme is better since it "exercises" the probe's characteristics in many directions, making the d_e value more correct for a general measurement.

2.6 Advantages of Using Coordinate Measuring Machine

Some of the advantages of using CMMs over conventional gaugging techniques are flexibility, reduced setup time, improved productivity.

2.6.1 Flexibility

Coordinate measuring machines are essentially universal measuring machines and do not need to be dedicated to any single or particular measuring task. They can measure practically any dimensional characteristic of virtually any part configuration, including cams, gears, and contoured surfaces. No special fixtures or gauges are required; because electronic probe contact is light, most parts can be inspected without being clamped to a surface plate.

2.6.2 Reduced Setup Time

Establishing part alignment and appropriate reference points are very time consuming with conventional surface-plate inspection techniques. These procedures are greatly simplified or virtually eliminated through software available on computer-assisted or computer-controlled CMMs.

Such software allows the operator to define the part's orientation on the CMM, and all coordinate data are subsequently automatically corrected for any misalignment between the part reference system and the machine coordinates. A CMM with sophisticated software can inspect parts in a single setup without the need to orient the part for access to all features even when a fourth axis (rotary table) is employed.

2.6.3 Improved Accuracy

All measurements on a CMM are taken from a common geometrically fixed measuring system, eliminating the introduction and accumulation of errors that can result with hard gage inspection methods and transfer techniques. Moreover, measuring all significant features of a part in one setup prevents the introduction of errors due to setup changes.

2.6.4 Reduced Operator Influence

The use of digital readouts eliminates the subjective interpretation of readings common with dial or venire-type measuring devices. Operator "feel" is virtually eliminated with modern electronic probe systems. All CMMs have canned software routines for typical part features, such as bores or center distances. In the part-program-assisted mode, the operator positions the machine; once the initial position has been set, the machine is under the control of a program that eliminates operator choice. In the computer numerically controlled (CNC) mode, motor-driven machines run totally unattended by operators. Also, automatic data recording, available on most machines, prevents errors in

transcribing reading to the inspection report. This all adds up to the fact that less skilled operators can be readily instructed to perform relatively complex inspection procedures.

2.6.5 Improved Productivity

All the factors previously mentioned help to make CMMs more productive than conventional inspection techniques. Further dramatic productivity improvements are realized through the computational and analytical capabilities of associated data handling systems, including calculators and all levels of computers.

2.7 The Review of Research about CMMs

2.7.1 Case 1 (Roundness Error)

The research of the roundness error presents a computational geometry based method of determining the roundness of a measured workpiece. A roundness error is evaluated with reference to ideal geometric features (i.e., a pair of ideal concentric circles), which must be established from actual measurements. The problem is defined as follows. A set S of n points $(P_1, P_2, P_3, \ldots, P_n)$ in a plane being given for $n \geq 4$ (for $n < 4$, the minimum separation of the pair of concentric circles from the n points can always be found to be zero) finds a pair of concentric circles C_1 and C_2 with the minimum radial separation SEP such that no point is exterior to the space bounded by the two circles.

Condition;

(1) Minimize SEP = $R_1 - R_2$

(2) C_1 and C_2 are concentric

(3) S is contained between C_1 and C_2

(4) $R_1 \geq R_2 \geq 0$

where, R_1 and R_2 are the radii of C_1 and C_2, respectively.

The traditional shop-floor method for evaluating a roundness error is by V-block measurements. The minimum radial separation between the concentric circles cannot be established directly by this method. In the ANSI standard, three methods are suggested:

(a) The maximum inscribed-circle (MIC) method

(b) The minimum circumscribed-circle (MCC) method

(c) The least-squares circle (LSC) method

If a circle is drawn with any point on a medial axis as its center, the circle touches two or more edges of the simple polygon (generated from the measured points figure 1.7) This contact point on the edges is the nearest (compared with points on other edges) to the center point of the circle. However, the contact points may not be points belonging to the point set. Therefore, the inner circle may not pass through any point of the desired point set. The roundness error thus obtained would be large than it should be.

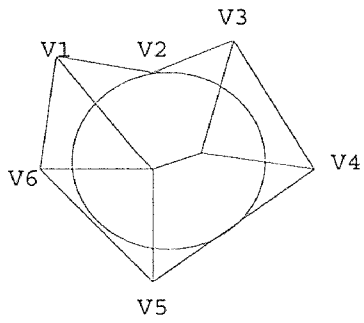

Figures 2.7 Medial Axes and Inscribe Circle

So that the correct ways of solving the geometric errors can be sought, it is necessary to mathematically formalize the geometric errors. The method for evaluating the roundness error is based on the computational-geometry-based techniques relating to convex-hull and Voronoi diagrams.

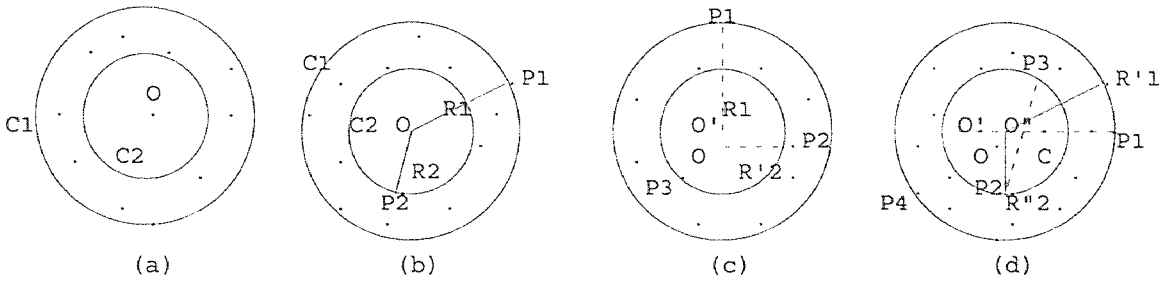

Figure 2.8 Each of the Circles Touches

Let C_1 and C_2 be any pair of concentric circles such that each point of S is properly inside the space bounded by C_1 and C_2 (see figure 2.8 (a)). With the same center, C_1 can still be enlarged while C_2 can be shrunk until each of the two touches at least one of the data points. Imagine that C_1 touches exactly on point P_1 of the data points while C_2 also touches exactly one data point P_2, so that all the other points are still bounded by the two circles (see figure 2.8 (b)).

From condition (1), evidently a decrement of SEP can be achieved by a decrease in R_1 and/or an increase in R_2. Here, it is assumed that R_1 is constant. To satisfy conditions (2) and (3), the center O of the circles C_1 and C_2 can only be shifted along the arc of radius R_1 that is centered at P_1 (see figure 2.8 (c)). It can shift either towards point P_2 or away from P_2. When the center shifts away from P_2, R_2 becomes larger. Thus, it results in a smaller SEP. The minimization of SEP proceeds until C_1 or C_2 touches one more point. As an example, in figure 2.8 (c), the shifting of center O continues until C_2 hits another point P_3. This step provides a new center O' and a new radius R'_2 of the inner circle.

Under conditions (2) and (3), center O' can still be shifted along the bisector of P_2P_3 to change SEP as shown in figure 2.8 (d). The center can move in either of the directions, towards or away from point C, from O'. Point C is the center of the circle passing through three points P_1, P_2 and P_3. As center O' moves towards point C, SEP is decreased. This is shown in figure 2.9.

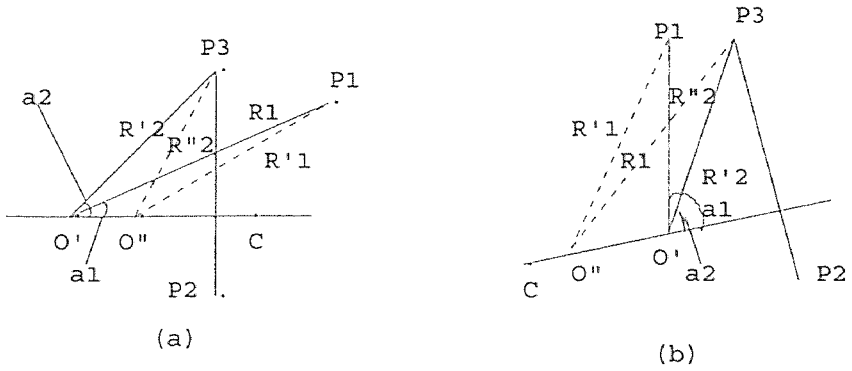

Figure 2.9 Calculation of Change of SEP Towards C

Depending on the location of the point P_1, two cases arise: Case (a), in which point P_1 lies on the right-hand side of the line that passes through P_2 and P_3, and (b), in which point P_1 lies on the left-hand side of the line. For (a), $\Delta R_1 = O'O''\cos\alpha_1$ and $\Delta R_2 = O'O''\cos\alpha_2$. When O'O" is small, $R'_1 \approx R_1 - \Delta R_1$ and $R''_2 \approx R'_2 - \Delta R_2$.

$$SEP'' = R'_1 - R''_2$$
$$\approx (R_1 - R'_2) - (\Delta R_1 - \Delta R_2)$$
$$= SEP' - (\Delta R_1 - \Delta R_2)$$

as $\alpha_2 > \alpha_1, \Delta R_1 > \Delta R_2$. Thus SEP" < SEP'.

For (b), it can be seen that the point C lies on the left-hand side of the line passing through P_2 and P_3. In a similar way to that of (a), when the center O' of the concentric circles is shifted towards point C, the increment of the radius of the inner circle is more than that of the outer circles, resulting in smaller radial that of the outer circles, resulting in smaller radial separation of the concentric circles.

As the center shifts towards C, the separation of the concentric circles becomes smaller and smaller. The minimization procedure stops when circle C_1 or circle C_2 touches another point. In the example above of figure 2.8 (d), the outer circle touches P_4. The new center is O", and the new radii are R'_1 and R''_2.

Three distinct things may arise during this minimization procedure, as shown in figure 2.10. In the above example, each of the outer and inner circles passes through two

points (a). The other two possibilities are (b), in which the inner circle passes through three points and the outer circle passes through one point, and (c), in which the outer circle passes through three points and the inner circle passes through one point. In (b) and (c), as either the outer or the inner circle passes through three points, the center is fixed, and it has no degree of freedom for further movement. Therefore, no further minimization of the radial separation is possible.

In general, given n points ($P_1, P_2, \ldots, P_n$) ($n \geq 4$) in a plane, there exists a pair of concentric circles with minimum separation such that all the points are bounded by those circles. The circles pass through at least four data points, and there is at least one datum on each circle. If an exhaustive ad hoc technique is used to find the concentric circles (with minimum radial separation) with any four points out of n data points being considered at a time, there is a risk of running into the danger of computational explosion. The computational complexity of this method is O (n). To overcome the drawback of the method, a much more efficient method is provided below. It is based on a computational-geometry technique.

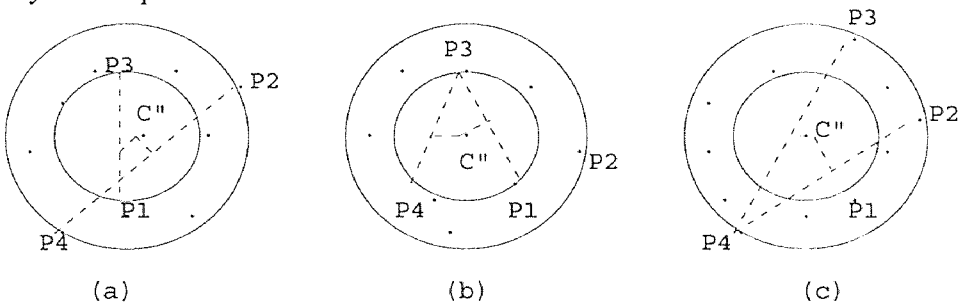

Figure 2.10 Three Cases of Concentric Circles for Roundness Error

The principles and procedure of this method are as shown in the flowchart shown in figure 2.11. The input to the system is the point set S obtained from the measured workpiece profile (on a cross-sectional plane that is perpendicular to the rotational axis). If the initial point set is arbitrarily measured, it is required to be sorted so that a simple polygon is generated from the data points. The sorting can be completed in the time of

O(n log n). It is then necessary to establish pairs of concentric circles for all three cases, and to select the desired pair with minimum separation. A brief discussion of the procedure follows.

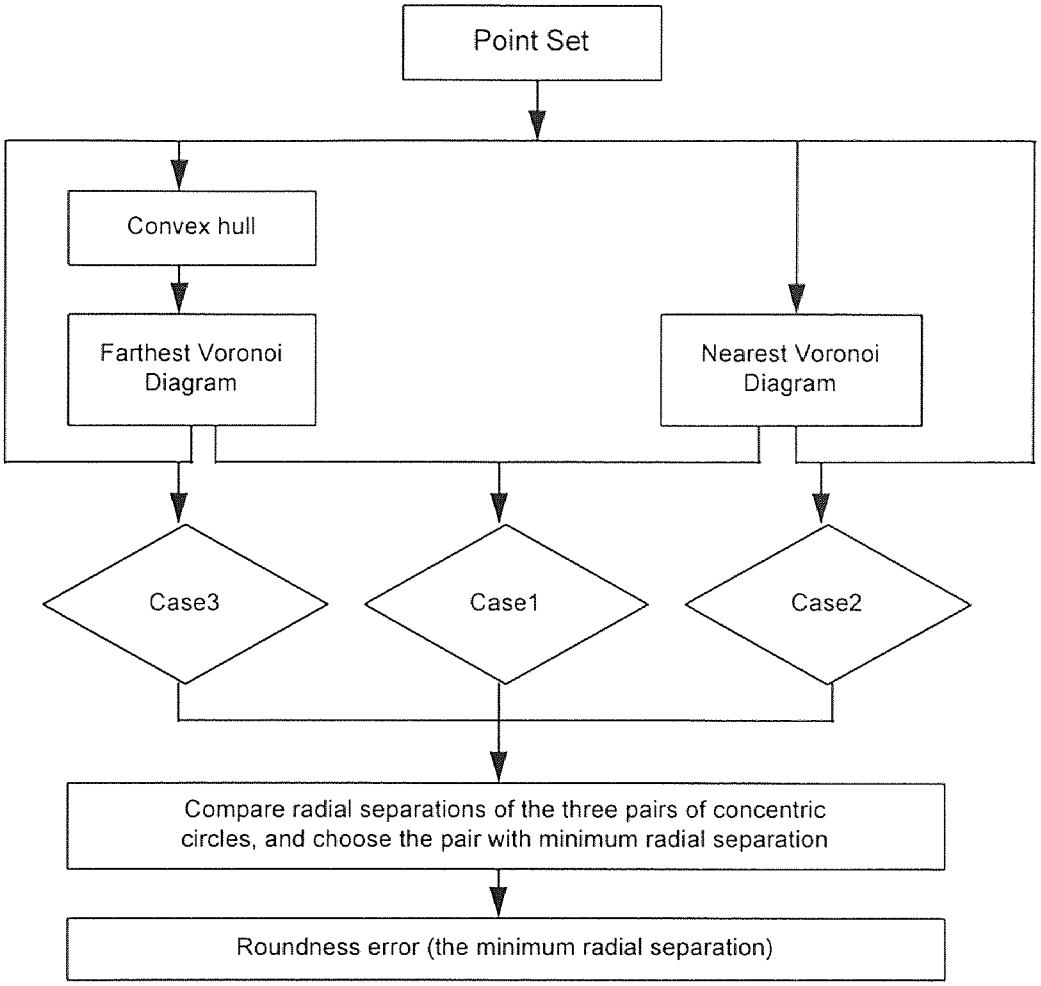

Figure 2.11 Flowchart for Calculation of Roundness Error

Step 1: Construct the convex hull CH(S) from the simple polygon. This step can be completed by the use of the Graham Scan method in O(n).

Step 2: Generate the Voronoi diagrams. The farthest Voronoi diagram FVor(S) is generated from the convex hull CH(S). The computational complexity is O(n log n). The

nearest Voronoi diagram NVor(S) is constructed from point set S. The computational complexity of constructing NVor(S) is the same as that for FVor(S)-O (n log n).

Step 3: Establish the pair of concentric circles with minimum separation for each of the three cases.

Case 1: Compute the intersection of FVor(S) and NVor(S), and obtain a set I_p of all the intersecting points of the two Voronoi diagrams. By Property 1, for every intersecting point $i_p \in I_p$, a pair of concentric circles centered at i_p can be constructed. The inner circle of the pair passes through at least two points of S nearest to the center i_p ; the outer circle passes through at least two points of S farthest from the center i_p. The concentric circles contain the whole point set S. The separation of the concentric circles is calculated. The $|I_p|$ pairs of such concentric circles can be generated in Case 1. The minimum separation SEP 1 of Case 1 is selected from the separations of all the pairs of concentric circles. As the computational complexity of calculating the intersections of E_N and E_F is O(n), the complexity may be further improved to O (n log n).

Case 2: Construct each pair P_c of concentric circles at every vertex v_n of V_N (the nearest Voronoi vertex set). By Property 1, therefore, the inner circle passes through at least three points (of S) that are nearest to the vertex v_n. The circle contains a set that is empty except for the points of S on the circle. The outer circle is determined by it being centered at v_n, and passing through a point of S that is farthest from the center v_n. For the vertex set V_N ,$|V_F|$ pairs of concentric circles are found. Their separations are calculated. The minimum separation, denoted by SEP2, is eventually selected from these separations for Case 2.

Case 3: In a similar way to that of Case 2, the concentric circles are constructed at vertices V_F. For each pair of the concentric circles, the radius r_1 of the outer circle is calculated, which is the distance from vertex v_f to any one of the three points that are farthest from v_f. The radius r_2 of the inner circle is the distance from vertex v_f to the point S that is nearest to v_f. The separation of the pair is obtained by subtracting r_2 from

r_1. A set of the separations is found that corresponds to set V_F. The minimum separation SEP3 of Case 3 is selected.

Step 4: If the results from the above-mentioned three cases are compared, the roundness error is determined as the minimum of SEP1, SEP2 and SEP3.

2.7.2 Case 2 (Circular Profiles)

The coordinates of the center of a sphere are determined "... arising from the position that the spherical center is the point for which the sum of the squares of distances from this point to points on a surface (which describe a sphere) is a minimum." On the basis of this strange definition, the author obtains for the center of the sphere, the center of mass of the measurement $X_o = \frac{1}{N}\sum X_i, \ldots, Z_o = \frac{1}{N}\sum Z_i$ the results of which are not at all valid: this can be seen by establishing the position of the Z-coordinate of the center when computed this way from measurements of only the upper hemisphere.

A method for an approximation to a general equation of a circle is suggested in [T. S. R. Murthy, 1986] which includes its presentation in the form

$$f(x,y) = A(x^2 + y^2) + ux + vy - 1 = 0$$

and the minimization of the functional $E(A,u,v) = \sum f^2(X_i, Y_i)$. A basic inadequacy of this algorithm is the fact that the position and radius of the given curve depend on the choice of system coordinates (in other words, on the choice of position of a feature in the field of a microscope or on the base of the machine). Omitting a deep, but simple proof of this assertion, let us look at only an obvious demonstration of this error. We determine a circle from some set of points X_i, Y_i and select a shift of the entire configuration so that the circle passes through the coordinate (0,0). An unfortunate normalization Equation (2.1) leads to a different circle since f (0,0) ≠ 0 for arbitrary A, u, and v. Thus, an attempt to repeat the computation for a new set of coordinates yields a problem that either becomes insoluble or gives a completely different circle.

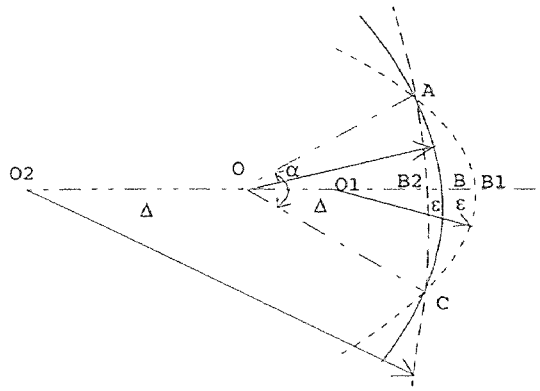

Figure 2.12 The View of Coordinate Measurement of Circular Profiles

Algorithm A3:

The mean circle is constructed, based on conditions for a minimum of the sum of squared distances from N measurement points, X_i, Y_i to the circle of unknown center A, B and radius R:

$$\Phi_3(A,B,R) = \sum(\sqrt{(x_i - A)^2 + (Y_i - B)^2} - R)^2 \qquad (2.1)$$

This nonlinear program is solved by the well-known numerical method of linearizing the functional and iterating. Let A_1, B_1, R_1 be the first approximation to the desired quantities A, B, and R that minimize Φ_3. At the k-th iteration, $x_i = X_i - A_k, y_i = Y_i - B_k$, the coordinate's relative to the most recent approximation of the center, and the quantities $r_i = \sqrt{x_i^2 + y_i^2}, u_i = \cos\theta_i = \frac{x_i}{r_i}, v_i = \sin\theta_i = \frac{y_i}{r_i}, d_i = r_i - R_k$. One then finds the corrections a, b, and r to $A_k, B_k, R_k, (|a|,|b|,|r| << R)$.

Linearization of equation (2.1) yields

$$\tilde{\Phi}_3(a,b,r) = \sum[\sqrt{(x_i - a)^2 + (y_i - b)^2} - (R_k + r)]^2 \cong$$

$$\cong \sum\left(r_i\sqrt{1 - \frac{2ax_i}{r_i^2} - \frac{2by_i}{r_i^2}} - R_k - r\right)^2 \cong$$

$$\cong \sum(au_i + bv_i + r - d_i)^2$$

The condition for a minimum of Φ_3 gives rise or a system of linear equation for a,b,and r

$$\begin{cases} aS_{uu} + bS_{uv} + rS_u = S_{ud}; \\ aS_{uv} + bS_{vv} + rS_v = S_{vd}; \\ aS_u + bS_v + rN = S_d. \end{cases} \tag{2.2}$$

Having determined a, b, and r, $A_{k+1} = A_k + a, B_{k+1} = B_k + b, R_{k+1} = R_k + r$, and the procedure is respected until the desired accuracy are obtained (max(|a|,|b|,|r|)<ε~0.1μm).

Algorithm A2:

This algorithm involves finding a circle of fixed radius R_o through points X_i, Y_i where R_o is equal to the nominal or most probable value, that is, the minimization is for $\Phi_2(A, B) = \Phi_3(A, B, R_o)$. The algorithm proceeds just as in algorithm A3 with the only difference since the deviation r is set equal to zero. This leads to a system of two equations (three equations in the case of a sphere) for the accuracy of the center position at each iteration:

$$\begin{cases} aS_{uu} + bS_{uv} = S_{ud} \\ aS_{uv} + bS_{vv} = S_{vd} \end{cases}$$

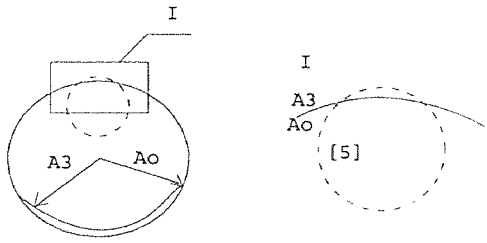

Figure 2.13 The Circular Profiles

Algorithm A1:

This algorithm concludes the series started with algorithms A3 and A2. It fixes the center position while varying only the radius. This is no different from the usual determination of mean radius for the distances from measured points to a nominal center position.

Algorithm A0:

This algorithm can be used in order to obtain a first approximation for algorithms A3 and A2. In it Φ_3 is "mapped" to a function Φ_0 that does not contain a radical:

$$\Phi_0(A,B,R) = \sum[(X_i - A)^2 + (Y_i - B)^2 - R^2]^2$$

Introducing the transformation $Q = R^2 - A^2 - B^2$, one finds $\tilde{\Phi}_0$, (A, B, Q) = Σ (2AX_i+ 2BY_i + Q - R_i^2)^2, where $R_i^2 = X_i^2 + Y_i^2$. The condition for a minimum $\tilde{\Phi}_0$ yields the following system of linear equations,

$$\begin{vmatrix} 2S_{xx} & 2S_{xy} & S_x \\ 2S_{xy} & 2S_{yy} & S_y \\ 2S_x & 2S_y & N \end{vmatrix} \times \begin{vmatrix} A \\ B \\ Q \end{vmatrix} = \begin{vmatrix} S_{rrx} \\ S_{rry} \\ S_{rr} \end{vmatrix} \qquad (2.3)$$

A rotation to the measurement center-of-mass coordinates system simplifies the solution of equation (2.3): S_x, S_y, and S_z become zero. Then $Q = S_{rr}/N$, A and B are determined from a system of two equations, $R = \sqrt{A^2 + B^2 + Q}$, and A and B are then translated back to the initial coordinate system.

Now let us look at the system of coordinates in which an arc of a circle with angle α is distributed symmetrically on both sides of the abscissa. We determine R_0 according to algorithm A0. The coefficients in equation (2.2) are substituted with their mean values, which are designated by the symbol s. From the conditions for a minimum of $\Phi_0, \sum(r_i^2 - R_0^2) = \sum((R_0 + d_i)^2 - R_0^2) = 0$, from which $s_d = -s_{dd}/(2R_0) \cong \sigma^2/(2R_0)$ where σ is the standard deviation. If the points are distributed approximately uniformly on the arc, an estimate for S_u from the mean value of the cosine becomes,

$$S_u = \frac{1}{\alpha}\int_{-\alpha/2}^{\alpha/2} \cos\theta d\theta = \frac{\sin(\alpha/2)}{\alpha/2} = \omega$$

Analogously, $S_{uu} = (1 + \omega\cos\alpha)/2, S_{vv} = 1 - S_{uu}, S_{uv} = 0, S_v = 0$ if d_i is distributed randomly and does not depend on angle, $S_{ud} \cong S_u S_d = \omega S_d, S_{vd} \cong S_v S_d = 0$. Then equation (2.2) takes the form

$$\begin{cases} aS_{uu} + r\omega = \omega S_d \\ bS_{vv} = 0 \\ a\omega^2 + r\omega = \omega S_d \end{cases} \tag{2.4}$$

from which it follows that a ≈ 0, b ≅ 0, $|r| \cong \frac{\sigma^2}{2R_0}$. Thus, for σ ≈ 100 μm and R ≈ 10 mm, r≈1 μm. That is, for microscopic deviations from circularity and macroscopic dimensions of features, algorithms A3 and A0 give practically the same value for the center coordinates, but show a difference in their values for a radius that is non negligible in comparison to the characteristic deviations of the order of σ. These estimates hold only for parameters of complete circles (apertures) or large arcs. For small α, equation (2.4) becomes poorly defined ($S_{uu} \to \omega^2, S_{vv} \to 0$) and lead to the divergence of algorithm A3. Therefore, we now examine the properties of data reduction for small arcs in more detail.

The illustrated in figure 2 is the displacement Δ of the center 0 of an arc defined by three points A, B, and C that result in a small displacement ε of point B. For ε << R, Δ ≅ ε × $\cot an^{-2}$ (α/4). This indicates that "in the allowed range ±ε" can be found in the arc of a circle, the scatter in the radius will exceed ε by many times.

The sensitivity of algorithm A0 to errors of measurement can be estimated by transforming the sum of equation (2.3) into integral form. The error ε for the point B gives the displacement of the center of the mean circle and is given by

$$\Delta = \frac{\varepsilon}{N} K(\alpha), where K(\alpha) = \frac{2(1-\omega)}{1+\omega\cos(\alpha/2) - 2\omega^2}$$

For arcs of 15, 30, 45, 90, 180, and 360°, K is equal to 440, 110, 50, 13, 4, and 2, respectively. A high sensitivity of the algorithms is mentioned in [G. A. Osokov and N. I. Chernov, 1984] as are their shortcomings. We consider that these are "shortcomings" of the geometrical properties of arcs and are thus inherently reflected in the algorithms.

The control of complex features by a coordinate measuring machine demands multiple replacement of the center position of a reference ball is measured, with the ball rigidly attached to the base of the machine. Usually just a part of the spherical surface, sometimes very small, is allowed for the probe that can lead to in adequacies in a table of

important operations with errors in the determination of the center position. To address this inadequacy, there is algorithm A2 in which the radius of the center position. To address this inadequacy, there is algorithm A2 in which the radius of the sphere is set equal to the sum of radii of the ball and head, both known with a high degree of accuracy.

The problem of comparing results of coordinate measurements is real, as far as differences in results obtained by various methods are significant. It is the opinion of the author that in the area of programmed and systematic resolution of these questions, the unified effort of many laboratories and the publication of defined, accepted standards and recommendations are necessary.

The simple algorithm A0 gives good initial approximations for various types of basic circles. The parameters are indistinguishable from values given by algorithm A3 that manifests the greatest rigor for the construction of a mean sphere. Unsatisfactory results for the reduction of measurements of small arcs are not from the inadequacy of the algorithms but, rather, from a defect in the method of reducing the measurements. In these cases, algorithm A2 is recommended for the construction of the base circle.

CHAPTER 3

THE CMM DEVIATION AS A FUNCTION OF THE NUMBER OF POINTS MEASURED

3.1 Determining Deviation from Circularity

When a point by point system is used to inspect a circle, then a minimum of three points is required to define the circle. The circle definition includes the radius of the circle, and the specific coordinates of its center point. Typically, in inspection we are looking for (i) eccentricity errors, and (ii) errors in the location of the center. As the number of points measured increases so does the likelihood that these error will be detected. Clearly, the only way we can be sure a circle is perfect, is by measuring an infinite number of points. Our objective is to measure the circle using the minimum number of points required to achieve a desired level of reliability. To do this we first need to define possible errors in eccentricity.

3.1.1 Circle Error

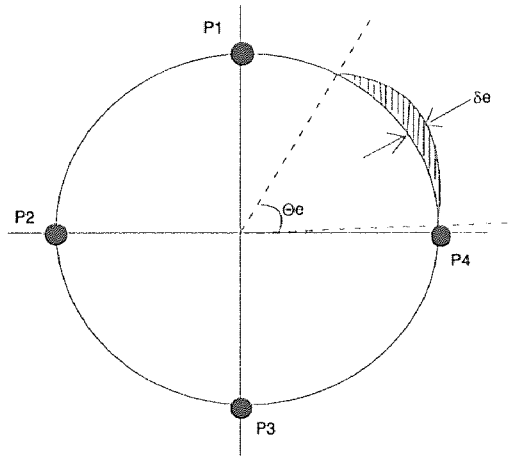

Figure 3.1 Standard Eccentricity Errors in a Circle

Any error in the eccentricity of a circle can be described as a departure from the true circle outline. Two parameters, Θe and δe, are measurable from each departure, where Θe is the cone angle of the error, δe is the maximum deviation of the error, respectively (see figure 3.1). Clearly, the ability to detect the error depends on the magnitude of Θe. When multiple errors are presented on the same circle, the smallest error will be the measuring countraint. To be able to analyze the errors, we must process (Θe, δe) and hence appropriately establish a measurement process. Alternatively, (Θe, δe) can be estimated from a historical data.

3.1.2 Selecting the Measurement Parameters

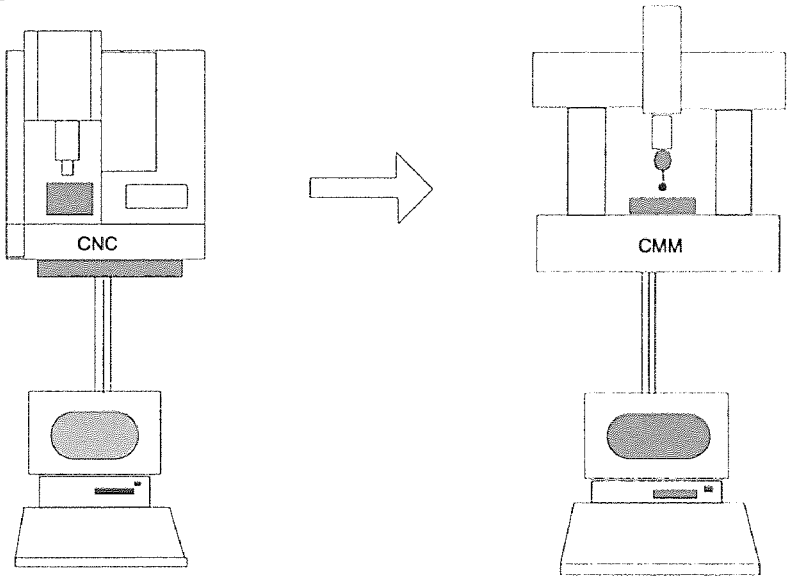

Figure 3.2 Facilities and System Integration

In figure 3.2, a circular geometry is made by a milling machine. The output is being inspected on a CMM. Let (Θmin, δmin) is the smallest error that could occur. To evaluate the circle, typically N equally spaced points are measured. If this means the angular distance between any two measured point is 360/N. Therefore Θmin < 360/N then it is quite possible that the error will go undetected.

$$\text{The probability of detecting the error} = \frac{\Theta_{min}}{360 / N}$$

When, $N \geq 360/\Theta min$ then we will in all certainty detect the error. Alternatively, if we are willing to accept a $\alpha\%$ of defect on average, and the expected production of defective parts is $\beta\%$, then

$$N = \frac{360}{\Theta_{min}}\left(1 - \frac{\alpha}{\beta}\right)$$

Deviations from circularity can be determined by knowing the actual deviations of the radial play of the measured rotations' bodies.

The radial play is the difference between the greatest and smallest distances from the points of the real profile of the rotation surface to the base axis in the cross section a plane perpendicular to this axis. It is known that deviations of radial play are composite deviations of shape and position of the working surfaces relative to the base surfaces, axes,etc., i.e., the components of deviations of radial play are deviations from circularity (shape deviations) and deviations that are functions of the location of the working surface relative to the base axis (location deviations), the fundamental cause of which is the presence of eccentricity (shifting of the base axis relative to the geometrical axis).

Radial play, which is a function only of eccentricity, in the absence of deviations from circularity, decreases smoothly along the circumference from the maximum value to zero.

By using these formulas, from the maximum radial play it is possible to calculate the radial play at given points through 45°. If the calculated values of radial play and the results of the measurement of radial play at the same points are known, then it is possible to determine the deviations characterizing the deviations from circularity as the difference between the calculated and the measured deviations of radial play.

In the presence of maximum radial play at any other point, for example at point 4, the opposite points 8 is taken as the initial one, i.e., the zero point, and at the remaining points the measurement results are recalculated to a magnitude equal to the measured

deviation at point 8 - a deviation that was observed at point 8 before it was taken as the zero point.

From this it may be concluded that the method under consideration can be used to measure deviations from circularity at a tolerance of more than 10 μm, when the error is equal to 5.4-9.1%, which is allowable. It is characteristic that on the average deviations from circularity are approximately 25% of the radial play, i.e., the primary deviations are deviations of radial play.

3.2 How to Measure Circle Using Least Squares Center by CMM

It is important that the source of measuring errors should, wherever possible, be determined and due allowance made for them in the measured size of the workpiece.

The alternative and recommended definition of roundness error are based on the least squares principle. When dealing with straightness, we have seen that it is possible to establish a unique datum line relative to a series of measured values by the principle of least squares. This enables both the slope and vertical intercept of the line to be established mathematically.

An analogous situation occurs in roundness measurement where we wish to establish a circle in relation to a series of measured values. In this case it is required to calculate the center of the least squares circle and also its radius and to use this as a datum from which to specify the errors of roundness.

3.2.1 Proof of the Formula for the Determination of the Least Squares Center and Circle

Consider a polar graph in rectangular coordinates x_i and y_i, originating at O, as shown in figure3.3. Take a number n of radii r_i, at equal angular spacing about O, which meet the trace at points given by ($r_i\theta_i$), where

$$\text{i=1,2,3, ... , n and } \theta_i = \frac{2\pi i}{n} \quad ,$$

Let the least squares circle have center C, whose rectangular coordinates are (a,b), and whose radius is R.

Let the distance from the origin O to the center C be c, and let the angle which OC makes with the x-axis be α.

Then,

$$c^2 = a^2 + b^2 \text{ and } \quad \tan\alpha = \frac{b}{a} .$$

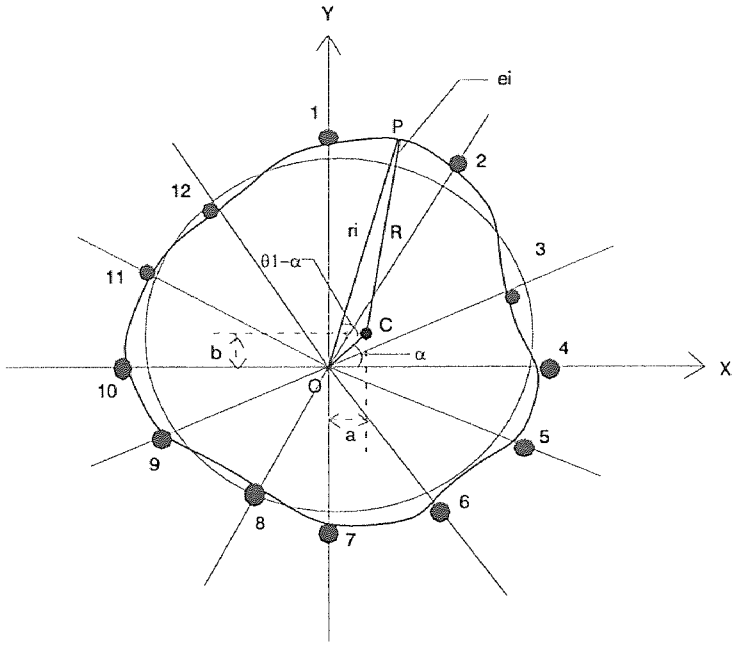

Figure 3.3 Diagram for Determination of the Least Squares Center

From the triangle OPC,

$$r_i = c\cos(\theta_i - \alpha) + \sqrt{(R + e_i)^2 - c^2 \sin^2(\theta_i - \alpha)}$$

where e_i is the deviation from the least squares circle along the radius r_i . Now in a well-centered trace c is very much less than R, and

$$r_i = c\cos(\theta_i - \alpha) + R + e_i \text{ approximately.}$$

By the principle of least squares $\sum e_i^2$ is a minimum, i.e., $\sum[r_i - R - c\cos(\theta_i - \alpha)]^2$ is a minimum, and so

$$\frac{\delta\sum e_i^2}{\delta R} = 0 \qquad \frac{\delta\sum e_i^2}{\delta c} = 0 \qquad \frac{\delta\sum e_i^2}{\delta \alpha} = 0$$

$$\frac{\delta\sum e_i^2}{\delta R} = -2\sum[r_i - R - c\cos(\theta_i - \alpha)] = 0$$

giving

$$\sum r_i - nR - c\sum\cos(\theta_i - \alpha) = 0 \tag{3.1}$$

$$\frac{\delta\sum e_i^2}{\delta c} = -2\sum[\cos(\theta_i - \alpha)(r_i - R - c\cos(\theta_i - \alpha))] = 0$$

giving

$$\sum r_i\cos(\theta_i - \alpha) - R\sum\cos(\theta_i - \alpha) - c\sum\cos^2(\theta_i - \alpha) = 0 \tag{3.2}$$

$$\frac{\delta\sum e_i^2}{\delta \alpha} = -2\sum[c\sin(\theta_i - \alpha)(r_i - R - c\cos(\theta_i - \alpha))] = 0$$

giving

$$\sum r_i\sin(\theta_i - \alpha) - R\sum\sin(\theta_i - \alpha) - c\sum\cos(\theta_i - \alpha)\sin(\theta_i - \alpha) = 0 \tag{3.3}$$

Expressing

$$\frac{\sum f(\theta)}{n} \text{ as } \frac{1}{2\pi}\int_0^{2\pi} f(\theta)d\theta$$

gives

$$\sum\cos(\theta_i - \alpha) = 0,$$

$$\sum\cos^2(\theta_i - \alpha) = \frac{n}{2},$$

and

$$\sum\cos(\theta_i - \alpha)\sin(\theta_i - \alpha) = 0$$

also

$$\sum r_i\cos(\theta_i - \alpha) = \cos\alpha\sum x_i + \sin\alpha\sum y_i = \cos\alpha n\bar{x} + \sin\alpha n\bar{y}$$

similarly,

$$\sum r_i\sin(\theta_i - \alpha) = \cos\alpha\sum y_i - \sin\alpha\sum x_i = \cos\alpha n\bar{y} - \sin\alpha n\bar{x}$$

Applying these results to equations (3.1), (3.2) and (3.3) give:

$$\sum r_i - nR - 0 = 0 \text{ from (3.1)}$$

i.e.,

$$R = \frac{\sum r_i}{n}$$

$$\cos\alpha n\bar{x} + \sin\alpha n\bar{y} - 0 - \frac{cn}{2} = 0 \quad \text{from (3.2)}$$

i.e.,

$$c = 2(\bar{x}\cos\alpha + \bar{y}\sin\alpha) \tag{3.4}$$

and

$$\cos\alpha n\bar{y} - \sin\alpha n\bar{x} - 0 = 0 \quad \text{from (3.3)}$$

i.e.,

$$\tan\alpha = \frac{\bar{y}}{\bar{x}} \quad .$$

Hence

$$\sin\alpha = \frac{\bar{y}}{\sqrt{(\bar{x}^2 + \bar{y}^2)}} \text{ and } \cos\alpha = \frac{\bar{x}}{\sqrt{(\bar{x}^2 + \bar{y}^2)}}$$

which substituted in (3.4) give

$$c = \frac{2(\bar{x}^2 + \bar{y}^2)}{\sqrt{(\bar{x}^2 + \bar{y}^2)}}$$

i.e.,

$$c = 2\sqrt{(\bar{x}^2 + \bar{y}^2)} \tag{3.5}$$

now

$$c = \sqrt{(\bar{x}^2 + \bar{y}^2)} \quad \text{and} \quad b = a\tan\alpha = \frac{a\bar{y}}{\bar{x}}$$

therefore

$$\sqrt{\left(a^2 + \frac{a^2\bar{y}^2}{\bar{x}^2}\right)} = 2\sqrt{(\bar{x}^2 + \bar{y}^2)} \quad \text{from (3.5)}$$

$$a\sqrt{\left(\frac{\bar{x}^2 + \bar{y}^2}{\bar{x}^2}\right)} = 2\sqrt{(\bar{x}^2 + \bar{y}^2)}$$

giving

$$a = 2\bar{x}$$

$$b = \frac{a\bar{y}}{\bar{x}} = 2\bar{y}$$

i.e.,

$$a = \frac{2\sum x_i}{n}$$

and

$$b = \frac{2\sum y_i}{n}$$

3.2.2 Example

Twelve equally spaced radial ordinates are drawn relative to the center of the chart and numbered 1 to 12 as shown in figure 3.3. The rectangular coordinates of the point of intersection between each ordinate and the polar diagram are measured with respect to the x and y axes, taking due account of sign.

These are tabulated, as shown in table 3.1, and the values of $\sum x$ and $\sum y$ used to establish the center of the least squares between each point of intersection and the least squares center may now be measured and used to calculate the radius of the least squares circle.

The roundness error is determined on the basis of the maximum peak to least squares circle plus maximum valley to least squares circle, which in the example shown in figure 3.3 equals 0.0010 in.

Table 3.1 Calculation of Least Squares Center and Radius

Position	x coordinate	y coordinate	radius
1	0	1.77	1.69
2	0.83	1.43	1.55
3	1.28	0.71	1.35
4	1.5	0	1.42
5	1.45	-0.8	1.64
6	0.73	-1.3	1.54
7	0	-1.3	1.33
8	-0.7	-1.1	1.4
9	-1.3	-0.7	1.16
10	-1.4	0	1.51
11	-1.1	0.63	1.37
12	-0.8	1.27	1.46
TOTAL	0.54	0.57	17.42

a = +0.0900 in. b = +0.0950 in. R = 1.4516 in.

3.3 Minimum Zone Evaluation

3.3.1 Straightness

Let S be the set of points in E^2. The convex hull H(s) of S is the smallest convex set containing S. A supporting line l of H(s) is a line passing through a vertex of H(s) such that the interior lies to one side the half-plane defined by line l.

Let Z(s) = $\{x \in E^2 \ / \ l_1 \geq x \geq l_2 \}$ be a zone, defined by l_1 and l_2, the two supporting parallel lines. The diameter,d, of Z(s) is the distance between the parallel supporting lines.

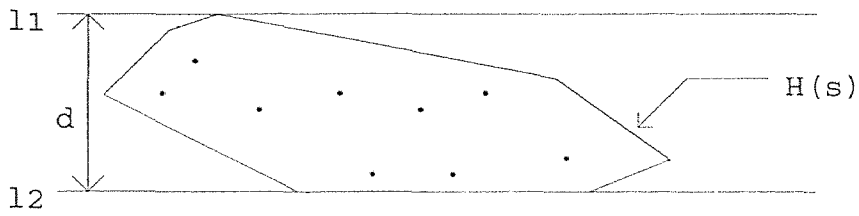

Figure 3.4 The Convex Hull H(s) of the Set of Points S

There are many such zones that can be defined, and the minimum zone is the zone with the smallest diameter.

$$d = l \times \sin\{\min(a_1, b_1), \max(a_2, b_2)\}$$

where, l = the length of the line joining the two points

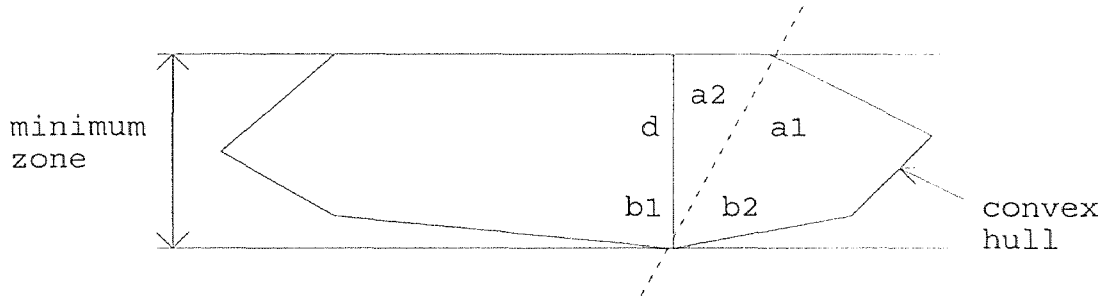

Figure 3.5 Convex Hull of Minimum Zone

The following algorithm can be used to determine the minimum zone.

Algorithm

1. Determine the convex hull H(s) of the set of points S.
2. For each edge ei of the convex hull (i=1,...,m)

   max distance = 0

   for each point Pj on the convex hull

   find distance dj of the point Pj from edge ei

if dj > max distance

then max distance + dj

next Pj

if max distance < min zone

then min zone = max distance

next ei

3.4 CMM Straightness

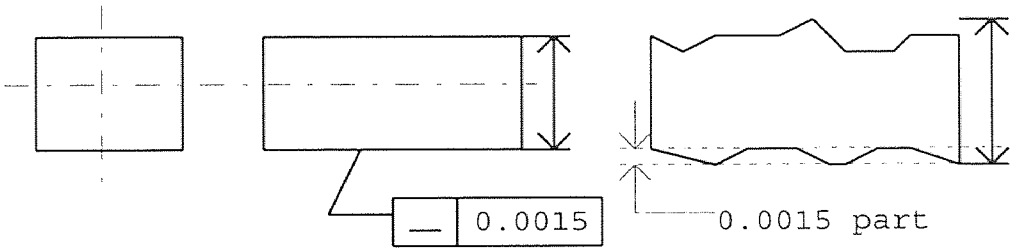

Figure 3.6 The Basic Diagram of Straightness Tolerance Zone

Form/straightness

This option computes the straightness of a line. The axis of the feature you are computing must fall within the straightness tolerance zone.

STR1 = FORM / STRAIGHTNESS ; line name

3.5 How to Measure Rectangle

It is often practical to express complex numbers z = x + i y in terms of polar coordinate's r, θ. These are defined by

$$x = r \cos \theta, \qquad y = r \sin \theta .$$

By substituting this we obtain the polar form of z,

$$z = r \cos \theta + i\, r \sin \theta = r (\cos \theta + i \sin \theta) .$$

r is called the absolute value or modules of z and is denoted by | z | . Hence

$$| z | = r = \sqrt{x^2 + y^2} = \sqrt{z\bar{z}} \quad .$$

Geometrically, | z | is the distance of the point z from the origin Figure3.10. Similarly, $|z_1 - z_2|$ is the distance between z_1 and z_2 figure 3.7 (b).

θ is called the argument of z and is denoted by arg z. Thus figure 3.7 (a)

$$\theta = \arg z = \arctan\frac{y}{x}$$

Geometrically, θ is the directed angle from the positive x-axis to OP in figure 3.7 (a) Here, as in calculus, all angles are measured in radians and positive in the counterclockwise sense.

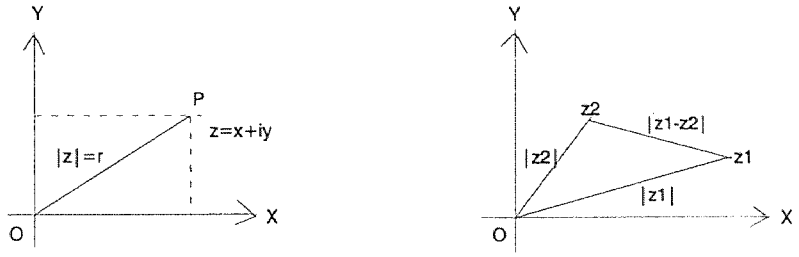

(a) (b)

Figure 3.7 Distance between Two Points in the Complex Plane

For z = 0 this angle θ is undefined. Why? For given $z \neq 0$ it is determined only up to integer multiples of 2π . The value of θ that lies in the interval $-\pi < \theta \leq \pi$ is called principal value of the argument of z ($\neq 0$) and is denoted by Arg z. Thus θ = Arg z satisfies by definition

$$-\pi < \text{Arg } z \leq \pi.$$

3.5.1 Experimentation

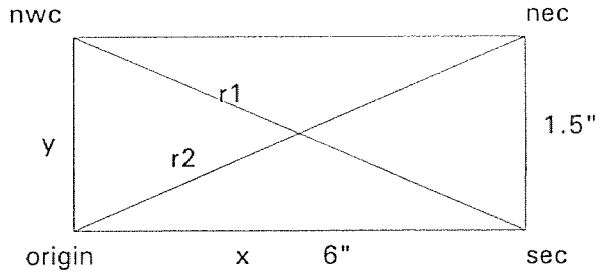

Figure 3.8 The Diagram of the Rectangle

The ideal cross-distance is 6.18466. ($r = \sqrt{x^2 + y^2}$)

Measured data :

This is the real distance between the North-West and South-East Corners.

r1 = 6.17984

This is the measured distance between the North-West and South-East Corners.

r1 = 6.17988

This is the real distance between the Origin and North-East Corners.

r2 = 6.18124

This is the measured distance between the Origin and North-East Corners.

r2 = 6.18151

We can calculate R distance by using triangle equation which is $R = \sqrt{x^2 + y^2}$. We can use this distance (R) when I'm measured the rectangle to compare with another rectangle.

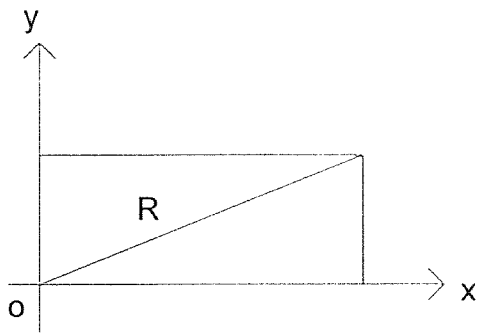

Figure 3.9 The Diagram of R Distance

To explain, how to measure, and how many points used to measure rectangle.

3.5.2 Procedure

1. To find the original point of rectangle two points of each line of the rectangle's side are measured using manually.

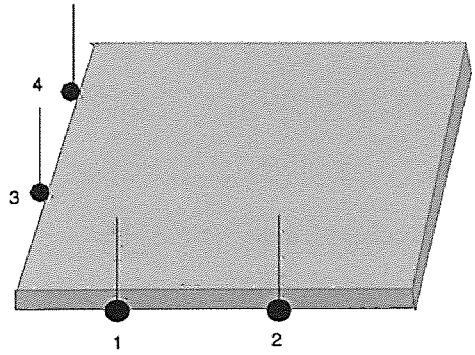

2. The CMM probe automatically touch to measure the location of orientation of the test two line of the rectangle side.

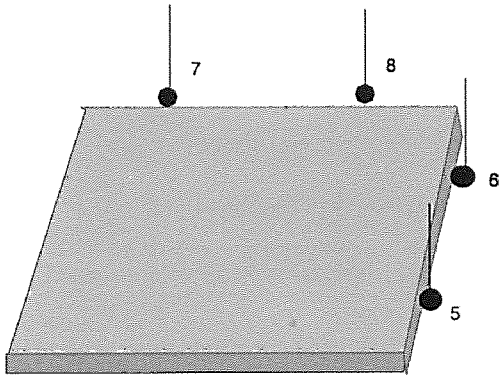

3. To calculate the distance (R) between the origin and the North East Corner (NEC),

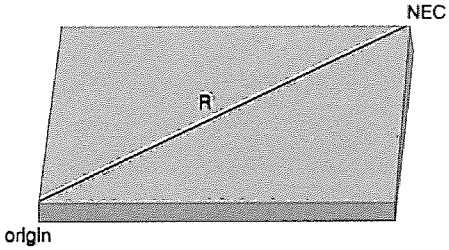

and then, I change the material on the CMM table. (Assuming that the material is under the mass production system.) and the probe touch one point to top's one line.

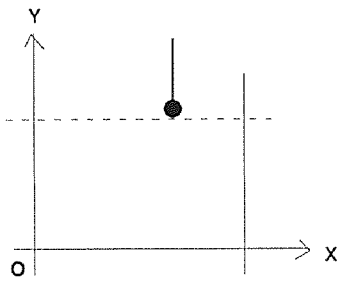

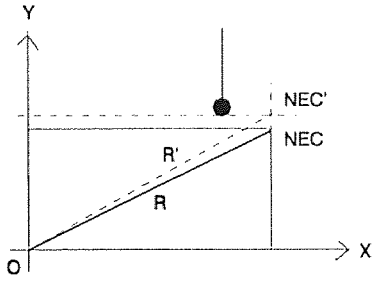

If the hitted point is higher than the original line, the NEC may moved to the point of NEC'. Now, the distance between the origin and NEC (R) is changed to R'.

4. To compare the original material and other material under the mass production system.
5. If the measured data (R') is different with R, then we reject this material in a confidence level of 95%. Interval is $P\left(R \pm Z\frac{\delta}{\sqrt{n}} \right) = 1-\alpha$. We assume that mass production system's material is normally distributed.

Table 3.2 The Distance (R) of Rectangle

number (times)	distance (R)
1	6.18151
2	6.18124
3	6.17984
4	6.18098
5	6.18132
6	6.18135

$$\overline{X} = 6.18104$$

$$s = \sqrt{\frac{\sum (X_i - \overline{X})^2}{n-1}} = \sqrt{\frac{(6.18151-6.18104)^2 + \cdots + (6.18135-6.18104)^2}{6-1}} = 0.000613$$

$$\Rightarrow 99\%$$

$$t_{0.005,5} = 4.032$$

$$P\left(6.18104 \pm 4.032\frac{0.000613}{\sqrt{6}}\right) = (6.18104 \pm 0.001009)$$

$$= (6.180031 \Leftrightarrow 6.182049)$$

$$\Rightarrow 95\%$$

$$P\left(6.18104 \pm 2.015\frac{0.000613}{\sqrt{6}}\right) = (6.18054 \Leftrightarrow 6.18154)$$

3.6 How to Measure Surface (Flatness)

Planes are measured by taking from 3 points on a surface. The direction of a plane is perpendicular to the plane and goes towards the direction from which the probe approached the part. The location of the plane is its centroid. The distance (d) is the perpendicular distance from the plane to the origin.

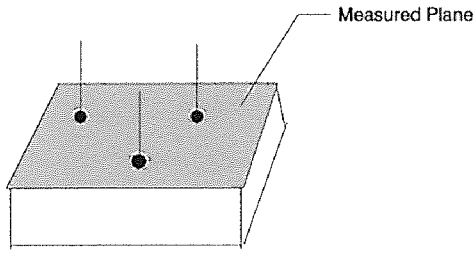

Figure 3.10 The Measuring of Surface

3.6.1 Least Squares Evaluation

The flatness tolerance from a set of coordinate points using the least squares technique. Given the form

$$z = ax + by + c$$

the following sum is minimized,

$$Min_{a,b,c} S = \sum e_i^2 = \sum (z_i - ax_i - by_i - c)^2$$

where a, b and c are determined by solving the following equations:

$$a\sum x_i^2 + b\sum x_i y_i + c\sum x_i = \sum x_i z_i$$
$$a\sum x_i y_i + b\sum y_i^2 + c\sum y_i = \sum y_i z_i$$
$$a\sum x_i + b\sum y_i + c\sum N = \sum z_i$$

This system is symmetric. To solve it for the unknown a, b and c. And where N is the number of sampled points. The distance of a sample point from the least squares plane is then given by

$$d_i = \frac{[z_i - (ax_i + by_i + c)]}{\sqrt{(1 + a^2 + b^2)}}$$

The flatness tolerance using the least squares approach is then :

Flatness tolerance = Max (di) - Min (di)

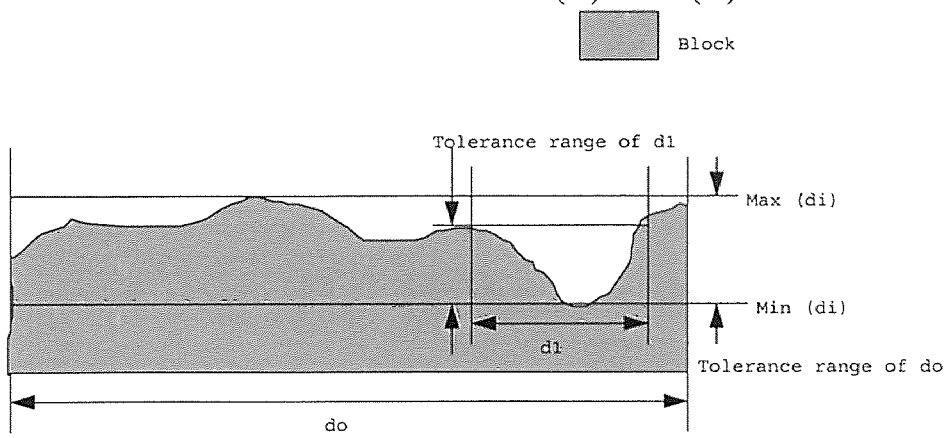

Figure 3.11 The Tolerance Range of Surface

Using the CMM, the flatness is measured as following: If I measured as distances d0, then I can find the tolerance ranges of d0. But the distance d1 is smaller than the distance d0, I couldn't find the same tolerance ranges of d0. The tolerance range of d1 is smaller than the tolerance range of do. Tolerance range depends on the distance.

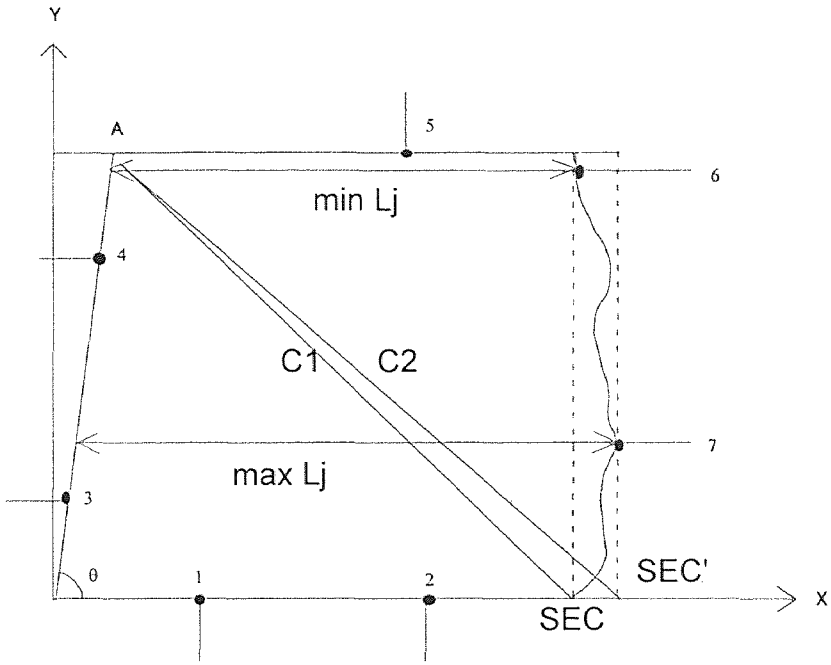

Figure 3.12 The Measured Point of the Rectangle

3.6.2 The Characteristics of the Aligned Rectangle

The CMM's probe touched minimum surface Lj which the minimum surface Lj is short length rectangle. The CMM computes the distance between the A point of figure 3.12 and SEC. The distance of C1, also the CMM calculate minimum Lj, which is called the minimum length. This is the distance between the Y-axis side. The side is parallel to it. Therefore, The optimization function is

$$\text{Min } T = \text{Max } (Lj) - \text{Min } (Lj) , \quad j = 1, 2, ..., N$$

where Lj is distance between the jth surface point and the straight line OA.

3.6.3 Angle

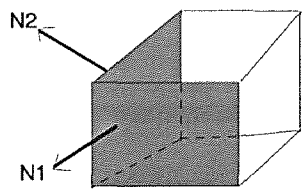

Figure 3.13 The Angle between Two Planes

The angle between two planes,

$$N1 = a_1 i + b_1 j + c_1 k \ , \qquad N2 = a_2 i + b_2 j + c_2 k$$

$$\cos\theta = \frac{N1 \cdot N2}{|N1| \cdot |N2|} = \frac{a_1 a_2 + b_1 b_2 + c_1 c_2}{|\sqrt{a_1^2 + b_1^2 + c_1^2}| \ |\sqrt{a_2^2 + b_2^2 + c_2^2}|} = \delta$$

$$\theta = \cos^{-1} \delta$$

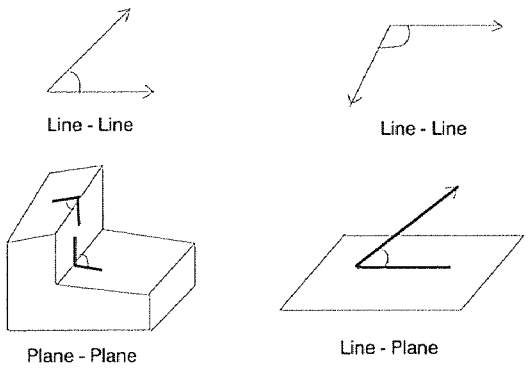

Figure 3.14 The Angle between Two Lines or Planes

The angle between two lines or two planes is the included angle between features; this angle is independent of the order in which features are entered. The angle between a line and a plane is the angle between the line and its projection to the plane. In the case of the line, which is perpendicular to the plane, this angle is reported as 90 degrees.

CHAPTER 4

ANALYSIS OF THE EXPERIMENTS

4.1 Objective and Procedure of the Experimentation

The purpose of this experiment is to find minimum points of the optimal range by using the Advanced Validator Interface Language (AVAIL™) of Coordinate Measuring Machine.

Two different alternatives to the Coordinate Measuring Machine Geometry Measurement Procedure (GMP/C) were studied.

* CMM rectangle geometry measurement procedure

* CMM circle geometry measurement procedure

CMM rectangle geometry measurement procedure refers to the situation where any rectangles are available for a measured data. This procedure evaluates the rectangularity of a rectangular part that should be at least a probe diameter in thickness and mounted parallel to the table.

CMM circle geometry measurement procedure also refers to the any circle. This circle program used for L-square analysis. At this point of the program will construct a point on a radius and angle that you will specify. This point will be the center for remeasurement of the origin circle.

In other words, the new "center" will be "off center" to provide a robust test of the integrity of the least squares evaluation can be achieved more safely and more simply by measuring a virtual circle that is eccentric to the physical circle and contained whinin the physical circle.

4.2 Statistical Analysis

Suppose that $X_1,\ldots,X_n$ is a sample from a normal population having unknown mean μ and unknown variance σ^2. We wish to construct a 100(1-α) percentage confidence interval for μ. Since σ is unknown, we can no longer base our interval on the fact that $[\sqrt{n}(\overline{X}-\mu)]/\sigma$ has a unit normal random variable. However, by letting $S^2 = \sum_{i=1}^{n}(X_i-\overline{X})^2/(n-1)$ denote the sample variance, then from $[\sqrt{n}(\overline{X}-\mu)]/S$ has a t distribution with n-1 degrees of freedom.

$$P\left\{t_{1-\alpha/2,n-1} < \sqrt{n}\frac{(\overline{X}-\mu)}{S} < t_{\alpha/2,n-1}\right\} = 1-\alpha$$

or , using that $t_{1-\alpha/2,n-1} = -t_{\alpha/2,n-1}$

$$P\left\{\overline{X} - t_{\alpha/2,n-1}\frac{S}{\sqrt{n}} < \mu < \overline{X} + t_{\alpha/2,n-1}\frac{S}{\sqrt{n}}\right\} = 1-\alpha$$

Thus, if it is observed that $\overline{X} = \overline{x}$ and $S = s$, then we can say that "with 100(1-α) percentage confidence"

$$\mu \in (\overline{x} - t_{\alpha/2,n-1}\frac{s}{\sqrt{n}}, \overline{x} + t_{\alpha/2,n-1}\frac{s}{\sqrt{n}})$$

Table 4.1 The Rectangle Results from Experimentation

TIMES	DIAG1	DIAG2	SEA	SWA
1	6.10483	6.09096	35.00772	34.7844
2	6.10224	6.09042	35.00041	34.7496
3	6.10502	6.09057	35.00245	34.7869
4	6.10333	6.09033	34.99915	34.76422
5	6.10384	6.0904	35.00013	34.77112
6	6.10418	6.09051	35.00161	34.77567
7	6.10407	6.09051	35.00158	34.77413
8	6.10429	6.09071	35.00431	34.77719
9	6.10428	6.09077	35.00517	34.77701
10	6.10416	6.09078	35.00533	34.7754
11	6.10423	6.09074	35.00478	34.77631
12	6.10416	6.09074	35.00466	34.77538
13	6.10416	6.09073	35.00461	34.77534
14	6.10414	6.09073	35.00456	34.77518
15	6.10413	6.09077	35.00511	34.775
16	6.10416	6.09076	35.00504	34.77543
17	6.10418	6.09073	35.00463	34.77571
18	6.10418	6.09074	35.00468	34.77573
19	6.10416	6.09078	35.00521	34.7754
20	6.10416	6.09079	35.0054	34.77537

The diagonal_1 ;

$$\overline{X} = 6.104095$$

$$s = \sqrt{\frac{\sum (x_i - \overline{X})^2}{n-1}} = \sqrt{\frac{(6.10483 - 6.104095)^2 + \cdots + (6.10416 - 6.104095)^2}{20-1}}$$

$$= 0.000544$$

95% confidence interval : $t_{\alpha/2,n-1} = t_{0.025,19} = 2.093$

$$P\left\{6.104095 - 2.093\frac{0.000544}{\sqrt{20}} < \mu < 6.104095 + 2.093\frac{0.000544}{\sqrt{20}}\right\}$$

$$= P\{6.10384 < \mu < 6.10435\}$$

The diagonal_2 ;

$$\overline{X} = 6.0906735$$

$$s = 0.0001593$$

95% confidence interval : $t_{0.025,19} = 2.093$

$$P\left\{6.0906735 - 2.093\frac{0.0001593}{\sqrt{20}} < \mu < 6.0906735 + 2.093\frac{0.0001593}{\sqrt{20}}\right\}$$

$$= P\{6.0905989 < \mu < 6.0907481\}$$

South East Angle ;

$$\overline{X} = 35.003827$$

$$s = 0.0021728$$

95% confidence interval : $t_{0.025,19} = 2.093$

$$P\left\{35.003827 - 2.093\frac{0.0021728}{\sqrt{20}} < \mu < 35.003827 + 2.093\frac{0.0021728}{\sqrt{20}}\right\}$$

$$= P\{35.0028101 < \mu < 35.0048439\}$$

South West Angle ;

$$\overline{X} = 34.7745095$$

$$s = 0.00730717$$

95% confidence interval : $t_{0.025,19} = 2.093$

$$P\left\{34.7745095 - 2.093\frac{0.00730717}{\sqrt{20}} < \mu < 34.7745095 + 2.093\frac{0.00730717}{\sqrt{20}}\right\}$$

$$= P\{34.77108968 < \mu < 34.77792932\}$$

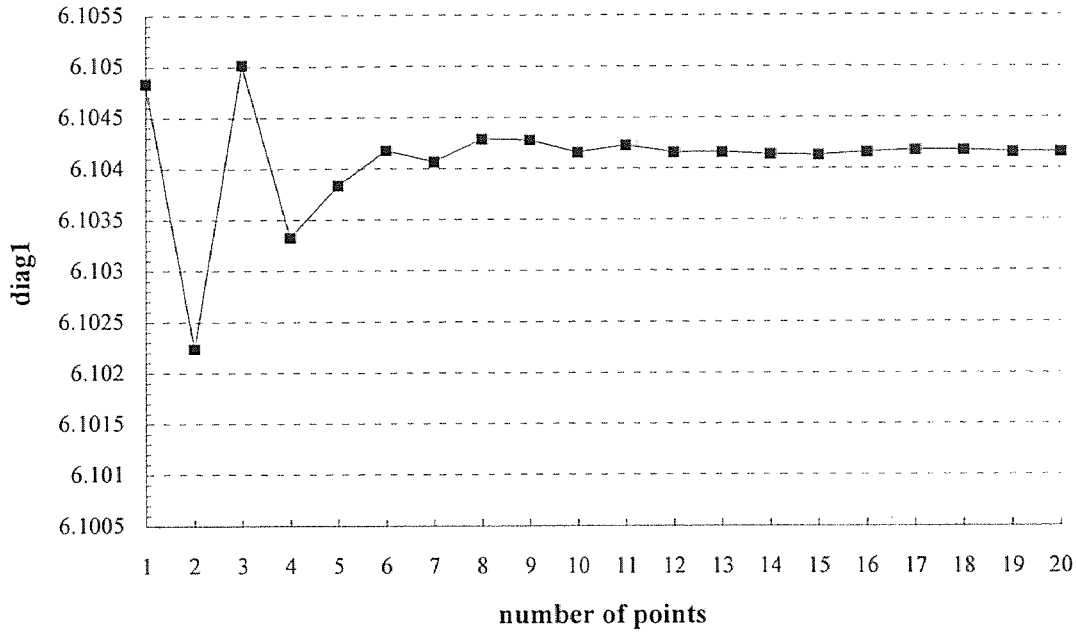

Figure 4.1 The Diagram of the Diagonal_1 Line

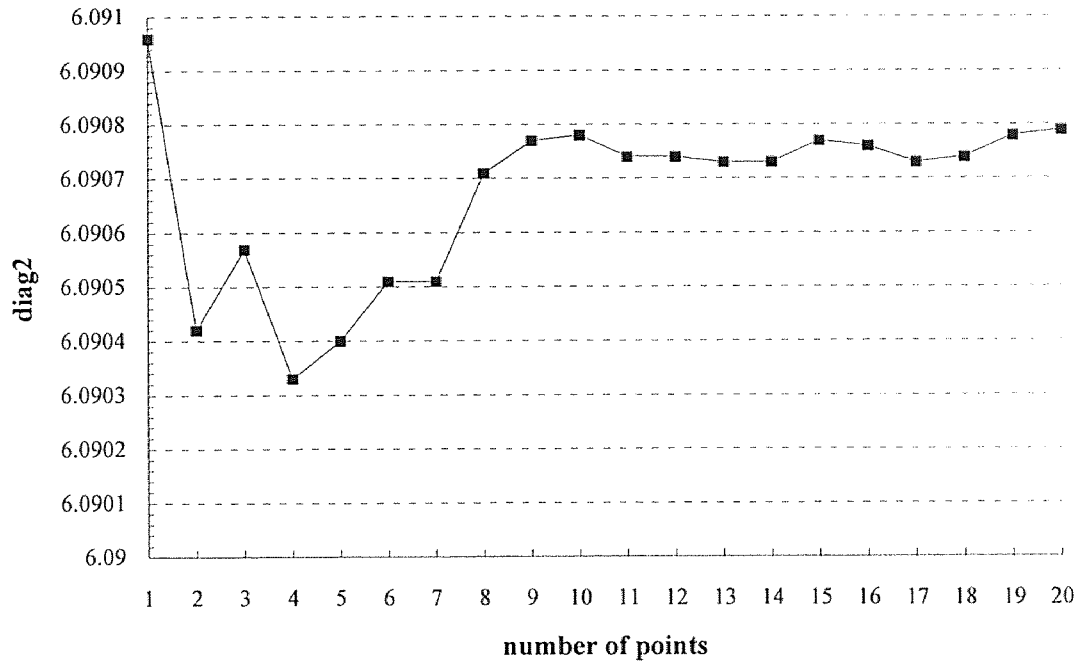

Figure 4.2 The Diagram of the Diagonal_2 Line

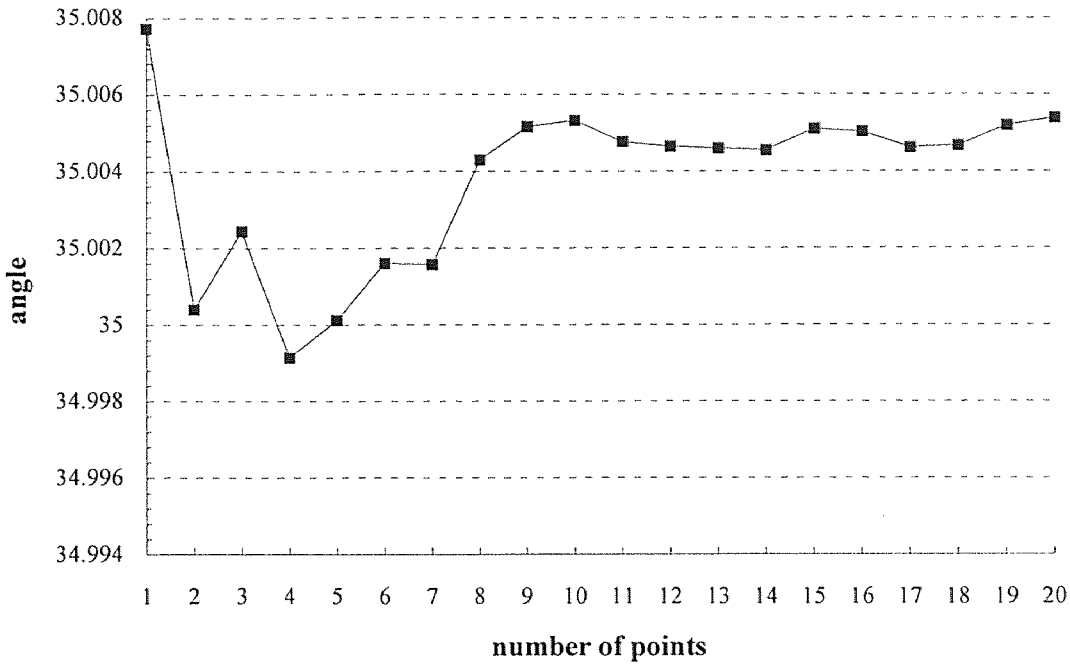

Figure 4.3 The Diagram of the South East Angle

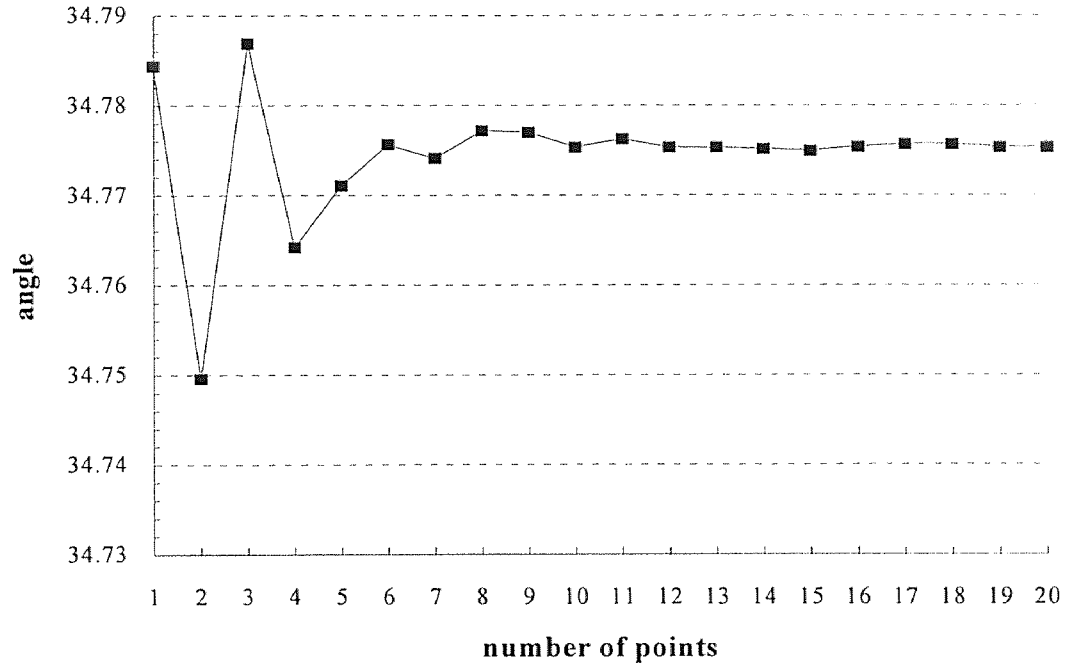

Figure 4.4 The Diagram of the South West Angle

Table 4.2 The Cast Results from Experimentation

# of point	A	B	R
3	0.24855	1.07525	1.53706
4	1.01337	0.0488	1.56093
5	0.84502	0.05357	1.5509
6	0.73418	0.05705	1.54501
7	0.65592	0.05853	1.54037
8	0.59725	0.05963	1.5368
9	0.5514	0.06094	1.5342
10	0.51411	0.06177	1.53207
11	0.4843	0.06235	1.53042
12	0.4597	0.06285	1.52877
13	0.43811	0.06327	1.5276
14	0.42017	0.06319	1.52642
15	0.40431	0.06428	1.52563
16	0.39057	0.06428	1.5249
17	0.37832	0.06461	1.52411
18	0.36768	0.0649	1.52348
19	0.35815	0.06496	1.52294
20	0.34938	0.06537	1.52252

Cast Radius ;

$\overline{R} = 1.533007$

$s = 0.010655$

95% confidence interval : $t_{\alpha,n-1} = t_{0.05,17} = 1.740$

$$P\left\{\mu < \overline{R} + t_{\alpha,n-1}\frac{s}{\sqrt{n}}\right\}$$

$$= P\left\{\mu < 1.533007 + 1.74\frac{0.010655}{\sqrt{18}}\right\}$$

$$= P\{\mu < 1.5373768\}$$

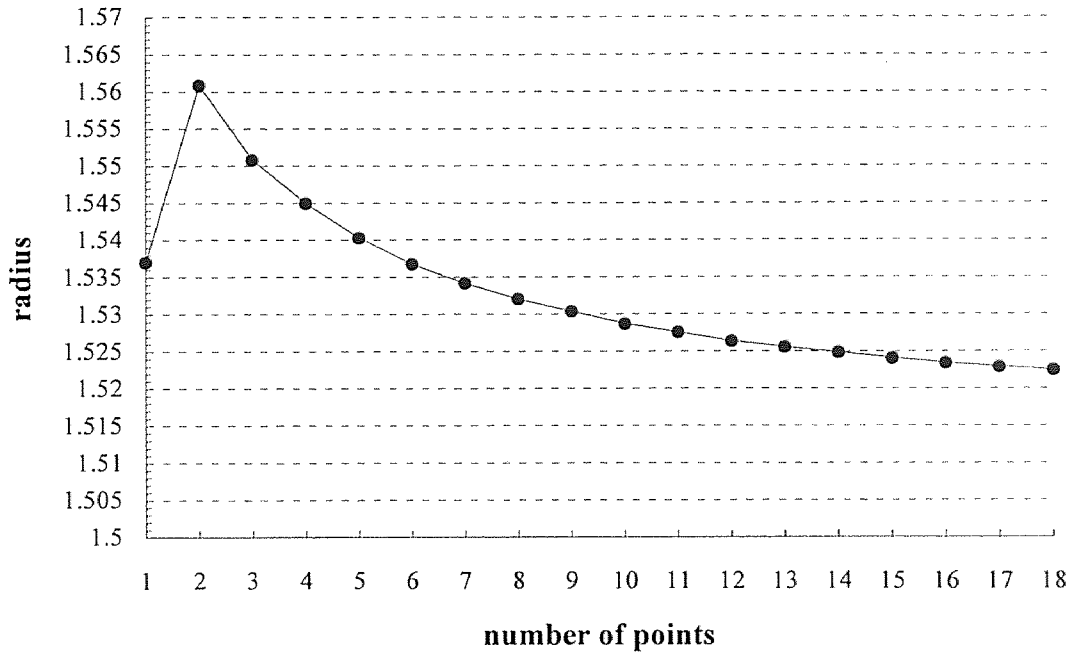

Figure 4.5 The Diagram of the Cast Radius

Table 4.3 The Tube Results from Experimentation

# of point	A	B	R
3	0.18548	0.92024	1.30764
4	0.83784	0.03828	1.32354
5	0.69713	0.04377	1.31663
6	0.60359	0.04587	1.31181
7	0.53727	0.04708	1.30847
8	0.48769	0.04811	1.30593
9	0.44813	0.04903	1.30398
10	0.41684	0.04963	1.3024
11	0.39167	0.04988	1.30109
12	0.37051	0.05063	1.30002
13	0.35252	0.05088	1.29911
14	0.33702	0.05143	1.29834
15	0.32397	0.05162	1.29764
16	0.31218	0.05185	1.29706
17	0.30195	0.05182	1.29654
18	0.29253	0.05214	1.29608
19	0.28457	0.05246	1.29568
20	0.2774	0.05239	1.29526

Tube Radius ;

$\overline{R} = 1.303179$

$s = 0.007906$

95% confidence interval : $t_{\alpha,n-1} = t_{0.05,17} = 1.740$

$$P\left\{\mu < \overline{R} + t_{\alpha,n-1}\frac{s}{\sqrt{n}}\right\}$$

$$= P\left\{\mu < 1.303179 + 1.74\frac{0.007906}{\sqrt{18}}\right\}$$

$$= P\{\mu < 1.3064214\}$$

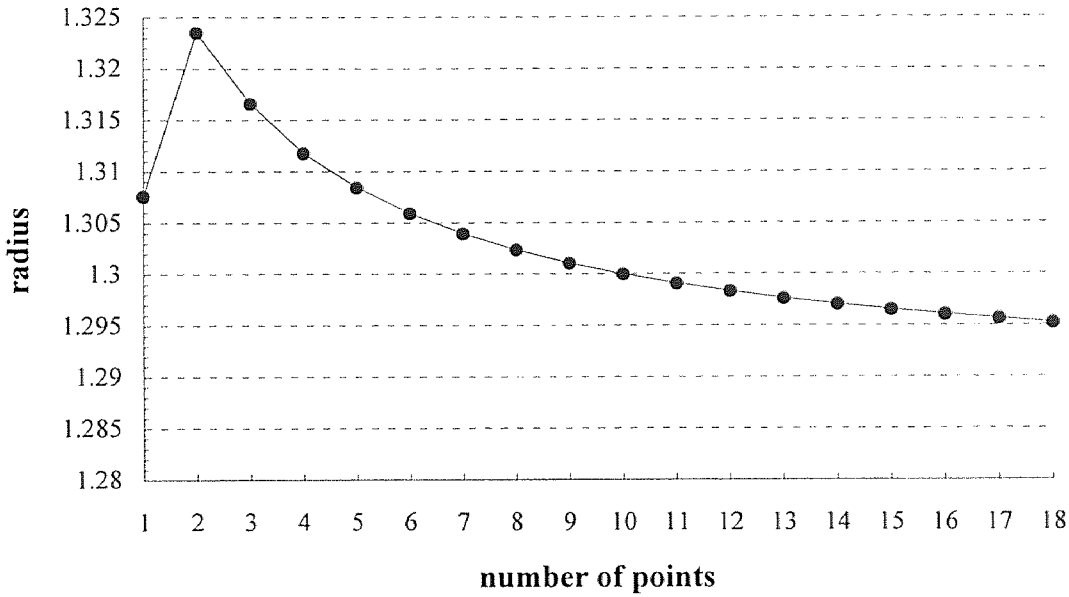

Figure 4.6 The Diagram of the Tube Radius

CHAPTER 5

CONCLUSION

This thesis offers a carefully matched range of measurement components and comprehensive customer support for production and quality control. Firsts of all, the most important things are short measuring time and high accuracy.

This thesis consists of CMM Geometry Measurement Procedure, a so called GMP/C, which represent independent functional process. Each procedure is a short but powerful process computer that solves the measurement and control tasks put to it.

The objectives of thesis are twofold. First, It is to find the geometric error in the material. Second, to optimize the number of points to be measured in an inspection that the requisite inspection information on the job in question is obtained in the minimum possible time.

The uncertainty of coordinate estimation is characterized by a variation interval associated with a specified confidence level. To reduce the influences of coordinate uncertainty on the accuracy of manufacturing and inspection, the propagation of coordinate uncertainty into the results of dimensional error evaluation and form tolerance evaluation is also studied.

The uncertainty analysis of coordinate estimation depends on the available information about the geometric errors on the part. At different stages of an inspection process, the available error information is different.

For inspection planning, since the detailed error information, such as the GMP/C of the geometric error at measurement points and the systematic component of form error is often not available. The statistical property of geometric errors is represented by the process capability in GMP/C analysis.

However, at the tolerance evaluation stage, more detailed information about the geometric error can be extracted from the measurement data and should be considered in tolerance evaluation.

APPENDIX A

PROGRAM FOR COORDINATE MEASURING MACHINE

This is the "oneshot" hits program that is automatically measurd rectangle.

```
!
!                       PC_AVAIL
!
!                     BROWN & SHARPE
!
!              ADVANCED VALIDATOR INTERFACE LANGUAGE
!
!FILENAME  : /USR/AVAIL/PART/KIM/LLF
!CREATED   : 16:09:57  18-JUNE-93
!
!
        VERSION/NUMBER;  2.900000
        UNITS/ENGLISH;
        OUTPUT/DEVICE; RECOUT
        QUALIFY/RECALL; TIPS
        QUALIFY/OLD_TIP; 1
        SETUP/PARAMETERS; 100.0,2,80,0.0917,0.0917,100.0,100.0,25
COUNT.SC2 = CALCULATION/COPY; 20
TEXT/DISPLAY; {
THIS PROGRAM EVALUATES THE "RECTANGULARITY" OF A
RECTANGULAR
PART WHICH SHOULD BE AT LEAST A PROBE DIAMETER IN THICKNESS
AND MOUNTED PARALLEL TO THE TABLE
}
TOP     = GEOMETRIC/PLANE;
        MANUAL/; 3
        DONE/;
TEXT/DISPLAY; {
THE EDGE ALONG THE FRONT WITH HITS TAKEN FROM LEFT TO RIGHT .....
}
FORX    = GEOMETRIC/2D_LINE; TOP
        MANUAL/; 2
        DONE/;
TEXT/DISPLAY; {
THE LEFT EDGE WITH HITS TAKEN FROM FRONT TO BACK .....
}
FORY    = GEOMETRIC/2D_LINE; TOP
        MANUAL/; 2
        DONE/;
FORO    = INTERSECT/POINT; FORX,FORY
        ALIGNMENT/PART; TOP,FORX,FORO,XYZ

WID.SC2 = TEXT/PROMPT; {
**************** PLEASE MOVE PROBE ABOVE PART ****************
```

```
WIDTH (a dimension in Y) IN INCHES
}
LEN.SC2 = TEXT/PROMPT; {
LENGTH (a dimension in X) IN INCHES
}
WINT1.SC2 = CALCULATION/DIVIDE; WID.SC2,3
WINT2.SC2 = CALCULATION/MULTIPLY; WINT1.SC2,2
LINT1.SC2 = CALCULATION/DIVIDE; LEN.SC2,3
LINT2.SC2 = CALCULATION/MULTIPLY; LINT1.SC2,2
WOFF.SC2  = CALCULATION/ADD; WID.SC2,0.5
LOFF.SC2  = CALCULATION/ADD; LEN.SC2,0.5


MOVE/TO; LINT1.SC2,WOFF.SC2,0

P1 = GEOMETRIC/POINT; YES
   MEASURE/; LINT1.SC2,WID.SC2,-PROBE.SC1,-YAXIS.I,-YAXIS.J,-YAXIS.K
   DONE/;
MOVE/TO; LINT2.SC2,WOFF.SC2,0
P2 = GEOMETRIC/POINT; YES
   MEASURE/; LINT2.SC2,WID.SC2,-PROBE.SC1,-YAXIS.I,-YAXIS.J,-YAXIS.K
   DONE/;

MOVE/TO; LOFF.SC2,WOFF.SC2,0
MOVE/TO; LOFF.SC2,WINT2.SC2,0

P3 = GEOMETRIC/POINT; YES
   MEASURE/; LEN.SC2,WINT2.SC2,-PROBE.SC1,-XAXIS.I,-XAXIS.J,-XAXIS.K
   DONE/;
MOVE/TO; LOFF.SC2,WINT1.SC2,0
P4 = GEOMETRIC/POINT; YES
   MEASURE/; LEN.SC2,WINT1.SC2,-PROBE.SC1,-XAXIS.I,-XAXIS.J,-XAXIS.K
   DONE/;

MOVE/BY; 0,0,1
MOVE/TO; 0,0,1

P_X = GEOMETRIC/2D_LINE; TOP
    RECALL/; P2
    RECALL/; P1
    DONE/;

P_Y = GEOMETRIC/2D_LINE; TOP
```

```
    RECALL/; P3
    RECALL/; P4
    DONE/;



SEC = INTERSECT/POINT; P_Y,FORX

TEXT/PRINTER; {

CHARACTERISTICS OF THE ALIGNED (INITIAL) RECTANGLE .....

}
PRINT_OPTION/AXES; XY
TEXT/PRINTER; {
THE COORDINATES OF NORTH WEST AND NORTH EAST CORNERS ARE

}
NWC = INTERSECT/POINT; FORY,P_X
NEC = INTERSECT/POINT; P_X,P_Y

PRINT_OPTION/AXES; D
        TEXT/PRINTER; {
THIS IS THE DISTANCE BETWEEN THE ORIGIN AND THE NORTH EAST
CORNER
}
DIAG1     = DISTANCE/2D; ORIGIN,NEC,TOP
        TEXT/PRINTER; {
THIS IS THE DISTANCE BETWEEN THE NORTH-WEST AND SOUTH-EAST
CORNERS
}
DIAG2     = DISTANCE/2D; NWC,SEC,TOP
PRINT_OPTION/AXES; DY
        TEXT/PRINTER; {
THIS IS THE DISTANCE BETWEEN THE XAXIS SIDE AND THE SIDE
PARALLEL TO IT
}
WIDTH     = DISTANCE/2D; FORX,P_X,TOP
PRINT_OPTION/AXES; DX
        TEXT/PRINTER; {
THIS IS THE DISTANCE BETWEEN THE YAXIS SIDE AND THE SIDE
PARALLEL TO IT
}
LENGTH    = DISTANCE/2D; FORY,P_Y,TOP
```

```
REMARK/; {
angle calculations
}
PRINT_OPTION/AXES;
L1 = GEOMETRIC/2D_LINE; TOP
   RECALL/; ORIGIN
   RECALL/; NEC
   DONE/;
L2 = GEOMETRIC/2D_LINE; TOP
   RECALL/; SEC
   RECALL/; NWC
   DONE/;

TEXT/PRINTER; {
THESE ARE THE ANGLES BETWEEN THE TWO DIAGONALS AND THE XAXIS
}
SEA = ANGLE/BETWEEN; L2,XAXIS
PRINT_OPTION/AXES; A
SEA.SC3 = CALCULATION/SUB; 180,SEA.SC3
SWA = ANGLE/BETWEEN; L1,XAXIS

PRINT_OPTION/AXES;



TEXT/PRINTER; {


SOME REPEATED MEASUREMENT .....

}



LEN.SC2  = CALCULATION/SUB; LEN.SC2,PROBE.SC1
MOVE/TO; PROBE.SC1,WOFF.SC2,1
MOVE/TO; PROBE.SC1,WOFF.SC2,-PROBE.SC1

        LOOP/TIMES; COUNT.SC2,2,1
INNER.SC2 = CALCULATION/COPY; LOOP.SC1

FLIP1.SC2 = CALCULATION/POWEROF; INNER.SC2,-1
INT.SC2  = CALCULATION/MULTIPLY; LEN.SC2,FLIP1.SC2
```

```
VAR1.SC2 = CALCULATION/COPY; PROBE.SC1
LOOP/TIMES; INNER.SC2,1,1
EL[] = GEOMETRIC/POINT; YES
    MEASURE/; VAR1.SC2,WID.SC2,-PROBE.SC1,-YAXIS.I,-YAXIS.J,-YAXIS.K
    DONE/;
VAR1.SC2 = CALCULATION/ADD; VAR1.SC2,INT.SC2
MOVE/TO; VAR1.SC2,WOFF.SC2,-PROBE.SC1
ENDOF/LOOP;
MOVE/BY; 0,0,1
MOVE/TO; PROBE.SC1,WOFF.SC2,1
MOVE/TO; PROBE.SC1,WOFF.SC2,-PROBE.SC1


PRINT_OPTION/AXES; Y
P_X = GEOMETRIC/2D_LINE; TOP
    LOOP/TIMES; INNER.SC2,1,1
    RECALL/; EL[]
    ENDOF/LOOP;
    DONE/;
PRINT_OPTION/AXES;

PRINT_OPTION/AXES; XY
TEXT/PRINTER; {
THE NEW COORDINATES OF NORTH WEST AND NORTH EAST CORNERS ARE

}
NWC = INTERSECT/POINT; FORY,P_X
NEC = INTERSECT/POINT; P_X,P_Y


PRINT_OPTION/AXES; D
        TEXT/PRINTER; {
THIS IS THE NEW DISTANCE BETWEEN THE ORIGIN AND THE NORTH EAST
CORNER
}
DIAG1    = DISTANCE/2D; ORIGIN,NEC,TOP
        TEXT/PRINTER; {
THIS IS THE NEW DISTANCE BETWEEN THE NORTH-WEST AND SOUTH-
EAST CORNERS
}
DIAG2    = DISTANCE/2D; NWC,SEC,TOP
PRINT_OPTION/AXES; DY
        TEXT/PRINTER; {
```

```
THIS IS THE NEW DISTANCE BETWEEN THE XAXIS SIDE AND THE SIDE
PARALLEL TO IT
}
WIDTH     = DISTANCE/2D; FORX,P_X,TOP
PRINT_OPTION/AXES; DX
        TEXT/PRINTER; {
THIS IS THE NEW DISTANCE BETWEEN THE YAXIS SIDE AND THE SIDE
PARALLEL TO IT
}
LENGTH    = DISTANCE/2D; FORY,P_Y,TOP

REMARK/; {
angle calculations
}
PRINT_OPTION/AXES;
L1 = GEOMETRIC/2D_LINE; TOP
   RECALL/; ORIGIN
   RECALL/; NEC
   DONE/;
L2 = GEOMETRIC/2D_LINE; TOP
   RECALL/; SEC
   RECALL/; NWC
   DONE/;

TEXT/PRINTER; {
THESE ARE THE ANGLES BETWEEN THE TWO DIAGONALS AND THE XAXIS
}
SEA = ANGLE/BETWEEN; L2,XAXIS
PRINT_OPTION/AXES; A
SEA.SC3 = CALCULATION/SUB; 180,SEA.SC3
SWA = ANGLE/BETWEEN; L1,XAXIS
PRINT_OPTION/AXES;

IFTEST/EQ; LOOP.SC1,LOOP.SC2,ENDL
TEXT/PRINTER; {

NEXT ITERATION .....
 }
ENDL = LABEL/;
        ENDOF/LOOP;
RESET/OUTPUT;
MOVE/BY; 0,0,1
MOVE/TO; 0,0,1
        ENDOF/PROGRAM;
```

APPENDIX B

PROGRAM FOR COORDINATE MEASURING MACHINE

This is the circle program by using least squares center method.

```
!                        PC_AVAIL
!
!                      BROWN & SHARPE
!
!              ADVANCED VALIDATOR INTERFACE LANGUAGE
!
!FILENAME  : /USR/AVAIL/PART/KIM1/LLF
!CREATED   : 11:59:38  18-JUN-93
!
!
        VERSION/NUMBER;   2.900000
        UNITS/ENGLISH;
        QUALIFY/RECALL; TIPS
        QUALIFY/OLD_TIP; 1
        SETUP/PARAMETERS; 100,2,80,0.0917,0.0917,100.0,100.0,25
OUTPUT/DEVICE; CIROUT
PRINT_OPTION/FORMAT; NONE
PRINT_OPTION/AXES;
        END.SC2 = CALCULATION/COPY; 20
REMARK/; {
minimum value for END.SC2 is 3
}
TEXT/DISPLAY; {
PLEASE MEASURE THE TOP PLANE OF THE SAMPLE PART
}
TOP      = GEOMETRIC/PLANE;
        MANUAL/; 3
        DONE/;

TEXT/DISPLAY; {
PLEASE MEASURE ANY CIRCLE ON THE SAMPLE PART:
1. The center will be the origin (for now)
2. The parameters of this circle will be used for the L-SQUARE analysis
}
FORO     = GEOMETRIC/CIRCLE; TOP
        MANUAL/; 3
        DONE/;
RLIM.SC2  = CALCULATION/MULTIPLY; FORO.SC1,0.97
        ALIGNMENT/PART; TOP,XAXIS,FORO,XYZ
ALIGNMENT/SAVE; THISONE,FIRST
```

```
THETA.SC2  = TEXT/PROMPT; {
AT THIS POINT THE PROGRAM WILL CONSTRUCT A POINT ON A RADIUS
AND ANGLE THAT YOU WILL SPECIFY. THIS POINT WILL BE THE "CENTER"
FOR REMEASUREMENT OF THE ORIGIN CIRCLE. IN OTHER WORDS, THE
NEW
"CENTER" WILL BE "OFF CENTER" TO PROVIDE A ROBUST TEST
OF THE INTEGRITY OF THE LEAST SQUARES CIRCLE ALRORITHM.

PLEASE ENTER SOME ARBITRARY ANGLE (DEGREES) VALUE .....
}
        TEXT/REPORT; RLIM.SC2,,,,,,,{
THIS VALUE IS 97% OF THE ORIGIN CIRCLE RADIUS
(also, please move probe above part)
}
        PAUSE/;
NOGOOD = LABEL/;
ZONE.SC1   = TEXT/PROMPT; {
PLEASE ENTER SOME RADIUS VALUE WHICH IS < OR = THE
PREVIOUSLY DISPLAYED VALUE (make it small) .....
}
        IFTEST/GT; ZONE.SC1,RLIM.SC2,NOGOOD

TEXT/PRINTER; {
THESE 60 XY VALUES ARE THE ORIGIN CIRCLE MEASURED WITH THE
"AUTO/CIR; ,,,,,,,," COMMAND.

    X       Y
}


BIGC    = AUTO/CIR; TOP,IC,60,0,0,-PROBE.SC2,FORO.SC2,0,360
        MOVE/TO; 0,0,1
        DONE/;
        BUFFER/DUMP; RAW
OUTPUT/USER_FORM; CIRPTS
PRINT_OPTION/FORMAT; USER
PRINT_OPTION/AXES; XY
LOOP/TIMES; 60,,
RP[]    = GEOMETRIC/POINT; YES
        RECALL/; RAW,LOOP.SC1,1
        DONE/;
ENDOF/LOOP;
PRINT_OPTION/FORMAT; NONE
PRINT_OPTION/AXES;
```

```
TEXT/PRINTER; {

LEAST SQUARES CIRCLE
*****************************************************

}

SIN.SC2   = FUNCTION/SINE; THETA.SC2
COS.SC2   = FUNCTION/COSINE; THETA.SC2
XX.SC2    = CALCULATION/MULTIPLY; ZONE.SC1,COS.SC2
YY.SC2    = CALCULATION/MULTIPLY; ZONE.SC1,SIN.SC2
ZZ.SC2    = CALCULATION/MULTIPLY; PROBE.SC2,-2
PP.X      = CALCULATION/COPY; XX.SC2
PP.Y      = CALCULATION/COPY; YY.SC2
PP.Z      = CALCULATION/COPY; ZZ.SC2
PP.TYP    = CALCULATION/COPY; 1

REMARK/; {
This "trick" is for safe measurement of the "off- center" circle....
(using the diameter of the real/physical origin circle)
The desired results for the least squares evaluation can be achieved
more safely and more simply by measuring a virtual circle which is
eccentric to the physical circle and contained within the
physical circle.
PP.SC2    = CALCULATION/COPY; FORO.SC2
SAFE.SC2  = CALCULATION/ADD; ZONE.SC1,0.05
        SETUP/PARAMETERS; 100.0,2,80,SAFE.SC2,SAFE.SC2,100.0,100.0,25

DP        = AUTO/CIR; TOP,IC,HITS.SC2,PP.X,PP.Y,PP.Z,PP.SC2,0,270
        MOVE/TO; 0,0,2.888
        DONE/;
}

PP2.X    = CALCULATION/MULTIPLY; FORO.SC1,COS.SC2
PP2.Y    = CALCULATION/MULTIPLY; FORO.SC1,SIN.SC2
PP2.Z    = CALCULATION/COPY; ZZ.SC2
PP2.TYP  = CALCULATION/COPY; 1

DDD       = DISTANCE/2D; PP,PP2,TOP
VC.SC2    = CALCULATION/MULTIPLY; DDD.SC2,2

NEWO      = PROJECTION/POINT; PP,TOP
ALIGNMENT/PART; TOP,XAXIS,NEWO,XYZ

REMARK/; {
```

```
MAIN LOOP
*****************************************************************
}
LOOP/TIMES; END.SC2,3,1
OUTPUT/USER_FORM; DIGIT
PRINT_OPTION/FORMAT; USER
PRINT_OPTION/AXES; R
COUNT.SC1 = CALCULATION/COPY; LOOP.SC1
PRINT_OPTION/FORMAT; NONE
PRINT_OPTION/AXES;

IFTEST/NE; LOOP.SC1,3,NORMAL
DP      = AUTO/CIR; TOP,IC,3,0,0,PP.Z,VC.SC2,0,180
          MOVE/TO; 0,0,1
          DONE/;
PTS = BUFFER/DUMP;
GOTO/LABEL; OKGO
NORMAL = LABEL/;

DP      = AUTO/CIR; TOP,IC,LOOP.SC1,0,0,PP.Z,VC.SC2,0,360
          MOVE/TO; 0,0,1
          DONE/;
PTS = BUFFER/DUMP;
OKGO = LABEL/;

EX.SC2 = CALCULATION/COPY; 0
EY.SC2 = CALCULATION/COPY; 0
ER.SC2 = CALCULATION/COPY; 0

TEXT/PRINTER; {

            X       Y       R
}
OUTPUT/USER_FORM; F_XYR
PRINT_OPTION/FORMAT; NONE

LOOP/TIMES; COUNT.SC1,,
PRINT_OPTION/AXES;
DP = GEOMETRIC/POINT; YES
   RECALL/; PTS,LOOP.SC1,1
   DONE/;
DR = DISTANCE/2D; PP,DP,TOP

EX.SC2 = CALCULATION/ADD; EX.SC2,DP.X
EY.SC2 = CALCULATION/ADD; EY.SC2,DP.Y
```

```
ER.SC2 = CALCULAITON/ADD; ER.SC2,DR.SC2

P[].X = CALCULATION/COPY; DP.X
P[].Y = CALCULATION/COPY; DP.Y

PRINT_OPTION/FORMAT; USER
PRINT_OPTION/AXES; XYR
P[].SC1 = CALCULATION/COPY; DR.SC2
PRINT_OPTION/AXES;

PRINT_OPTION/FORMAT; NONE

ENDOF/LOOP;

PRINT_OPTION/AXES;

TEXT/PRINTER; {

}
TOTAL.X = CALCULATION/COPY; EX.SC2
TOTAL.Y = CALCULATION/COPY; EY.SC2
PRINT_OPTION/FORMAT; USER
PRINT_OPTION/AXES; D
TOTAL.SC1 = CALCULATION/COPY; ER.SC2
TEXT/PRINTER; {

}
PRINT_OPTION/FORMAT; MEASURED
PRINT_OPTION/AXES;
EX.SC2 = CALCULATION/MULTIPLY; EX.SC2,2
EY.SC2 = CALCULATION/MULTIPLY; EY.SC2,2
RECIP.SC2 = CALCULATION/POWEROF; COUNT.SC1,-1
PRINT_OPTION/AXES; D
A.SC2    = CALCULATION/MULTIPLY; EX.SC2,RECIP.SC2
B.SC2    = CALCULATION/MULTIPLY; EY.SC2,RECIP.SC2
R.SC2    = CALCULATION/MULTIPLY; ER.SC2,RECIP.SC2
TEXT/PRINTER; {
**********************************************************************
******
 }
 ENDOF/LOOP;

RESET/OUTPUT;

        ENDOF/PROGRAM;
```

BIBLIOGRAPHY

1. ANSI B89.3.1-1972, *Measurement of out of roundness*, The American Society of Mechanical Engineers, New York, USA, (1972).

2. ANSI Y14.5M-1982, *Dimensioning and tolerancing*, The American Society of Mechanical Engineers, New York, USA, (1982).

3. Bowyer, A and Woodwark, J., *A Programmer's Geometry Butterworths*, UK, 1983.

4. Dewey, B. R., *Computer Graphics for Engineers,* Harper & Row, USA, 1988.

5. Foster, L. W., *GEO-METRICS II*, Addison-Wesley, USA, 1986.

6. Houle, M. E. and Toussaint, G. T., *Computing the width of a set*, IEEE Trans. Pattern Anal. & Machine Intell. Vol PAMI-10 No 5 (1988), pp. 761-765.

7. Lai, K. and Wang, J., *A computational geometry approach to geometric tolerances*, 16th North American Manufacturing Research Conf. (1988), pp. 376-379.

8. Lee, D. T., *Medial axis transformation of a planar shape*, IEEE Trans. Pattern Anal. & Machine Intell. Vol PAMI-4 No 14 (1982), pp. 363-369.

9. Oskov G. A. and Chernov N. I., *Efficient Algorithms for the Fitting of Circles*, Preprint P5-84-7, OIYaI, Dubna, 1984. (Russian)

10. Roy, U. and Zhang, X., *Assessment of geometric tolerances by computational geometry techniques*, Technical Report No 9005 CASE Center, Syracuse University, USA, (April 1990).

11. Samburskaya G. N., *Investigation of the Measurement of Geometrical Parameters of Surfaces*, Trudy VNIIMS (1988), p. 69. (Russian)

12. Scarr, A. J. T., *Metrology and Precision Engineering*, McGraw-Hill, UK, 1967.

13. Shunmugan, M. S., *New approach for evaluating form error of engineering surface*, Computer Aided Design, Vol 19 No 7 (1987), pp. 368-374.

14. Stanat, D. F. and McAllister, D. F., *Discrete Mathematics in Computer Science*, Prentice-Hall, USA, 1977.